Multi-scale Computational Modeling for Plasma Assisted Ignition and Combustion Control

Laxminarayan L. Raja
Dept. of Aerospace Engr. and Engr. Mech,
The University of Texas at Austin
Austin, Texas 78712

Online Low Temperature Plasma Seminar Series
(1st Nov 2022)

Outline

- Motivation for advanced combustion ignition concepts
- Trends in advanced Internal Combustion (IC) Engines
- Plasma-Assisted Ignition/Combustion (PAI/PAC) approaches
- Model and Computational Approach
- Examples
  1) Coaxial and Corona igniter
  2) Fast pulsed behavior of conventional spark plugs
  3) Insights from arc modeling in a spark plug
  4) New concept for SSPP-based wide-area surface plasma ignitor

Overarching goals for advanced combustion

- Control of emissions from combustion process

- Improved efficiency of combustion

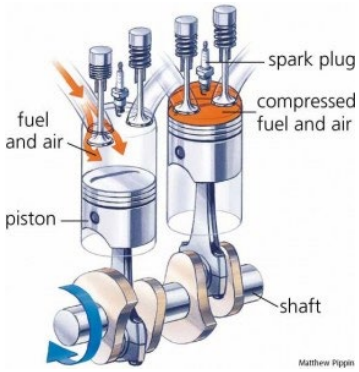

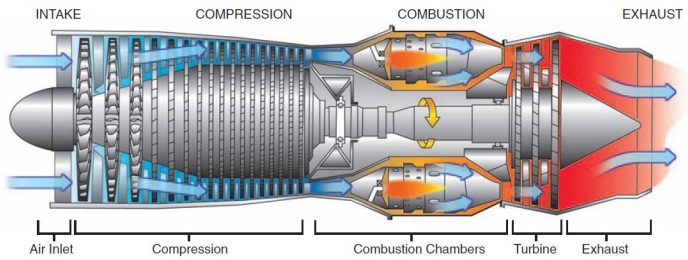

- Improved ignitability/reactivity of hard-to-burn fuels and in difficult combustion environments

Strategies for improved efficiency and lower emissions

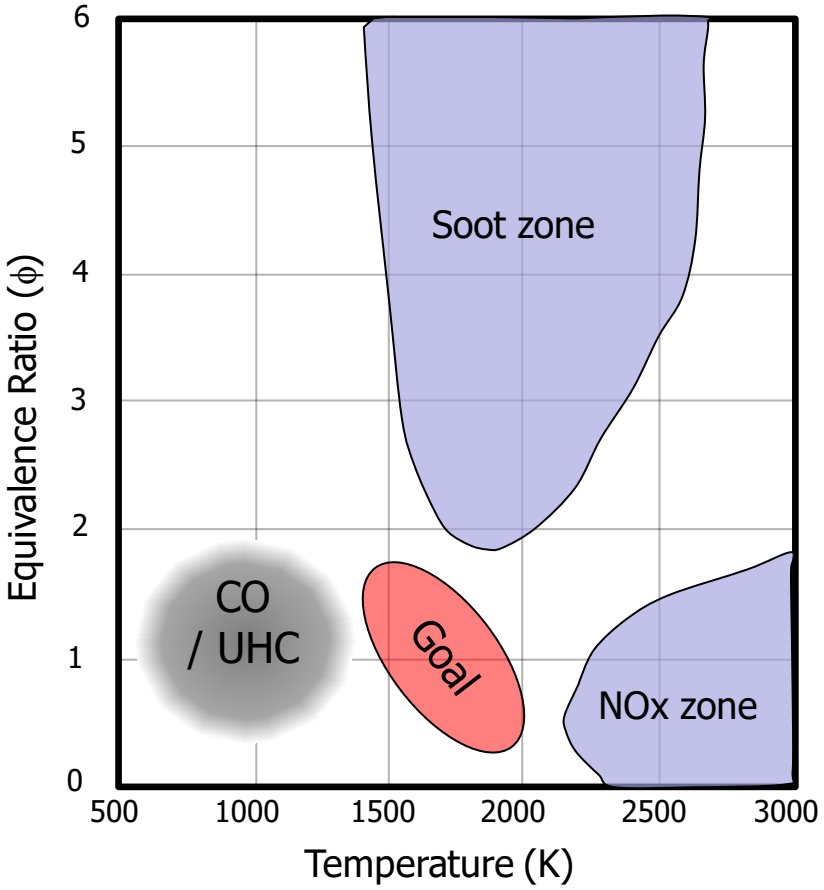

- Dilution to reduce adiabatic flame temp. to avoid NOx zone
- Lean F/A mixture (improved mixing prior to combustion) to avoid Soot zone
- High pressure to improve combustion efficiency

Emphasis of this talk will be on Internal Combustion Engine Ignition

Motivation for dilute (lean), high pressure combustion

$$\eta_{\text{Otto}} = 1 - \frac{1}{\text{CR}^{\gamma-1}}$$

- η_{Otto} ↑ → CR ↑ → $\frac{V_1}{V_2} = \left(\frac{p_2}{p_1}\right)^{1/\gamma}$ ↑ → **High pr. comb.**
- Dilution (air or EGR) → T_{ad} ↓
- T_{ad} ↓ → NOx ↓, Heat loss ↓
- η_{Otto} ↑ → γ ↑
- $\gamma \approx 1.4$ (air), $\gamma \approx 1.3$ (exhaust)
  → Air dilution preferable → **Lean comb.**

Dilution and high-pressure combustion is accompanied by a cost

- High pressures → Spark plug gap ↓ → Heat loss ↑

Cold plasma ?

Plasma-flow coupling ?

→ Plasma dimension ↓ → flame kernel probability ↓

- Dilute (Lean) F/A mixtures → Ignition limit

Plasma radical / thermal enhancement of ignition ?

→ s_L ↓ → flame kernel growth ↓

Plasma improvement of combustion reactivity ?

→ COV_{IMEP} ↑ (stability ↓)

→ T_{ad} ↓ → Unburned HC ↑

Advanced Ignition approaches seek to address above problems

Numerous plasma platforms available for PAI

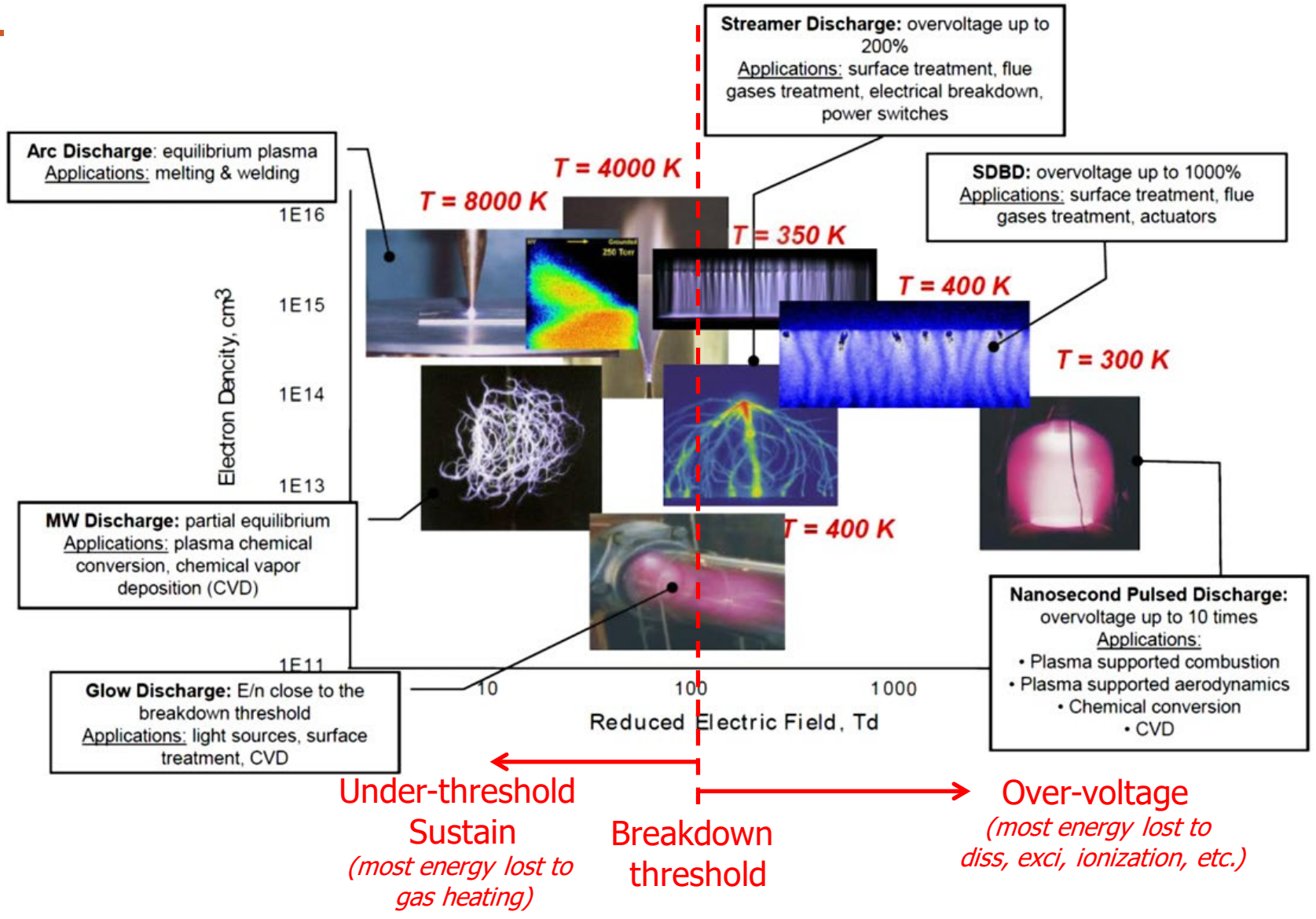

Starikovskiy and Alexandrosov, Prog. Energy Comb. Sci. 39, 61 (2013)

Several ignition approaches have been studied for IC engine ignition applications

Conventional spark plug (SI)

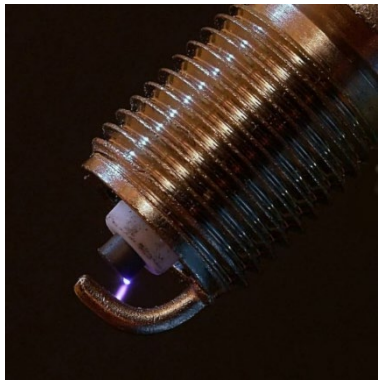

Dielectric Barrier (DBD)

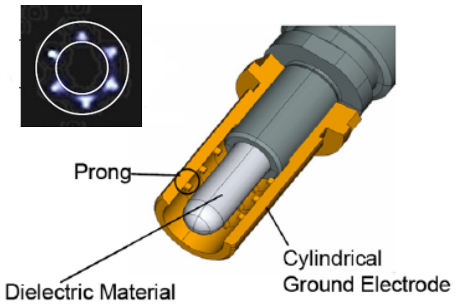

Shiraishi and Urushira (Nissan)

Nanosecond Pulsed (NSP)

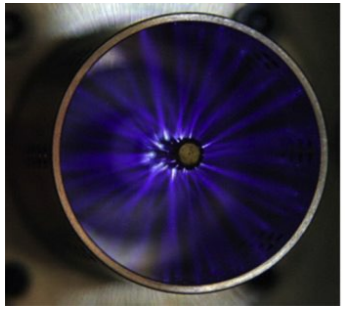

Nissan / Univ. S Cal.

NGK sparkplug

TPS Inc.

Laser spark plug

RF Corona

EcoFlash (BorgWarner)

ACIS (Federal Mogul)

Microwave enhanced SI

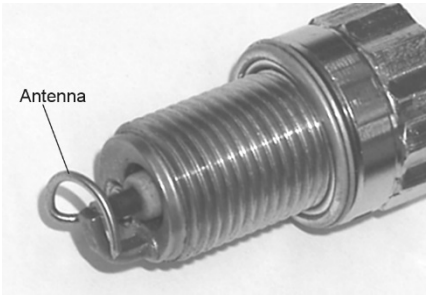

Imagineering Inc.

Overview of physical and chemical processes in PAI/PAC

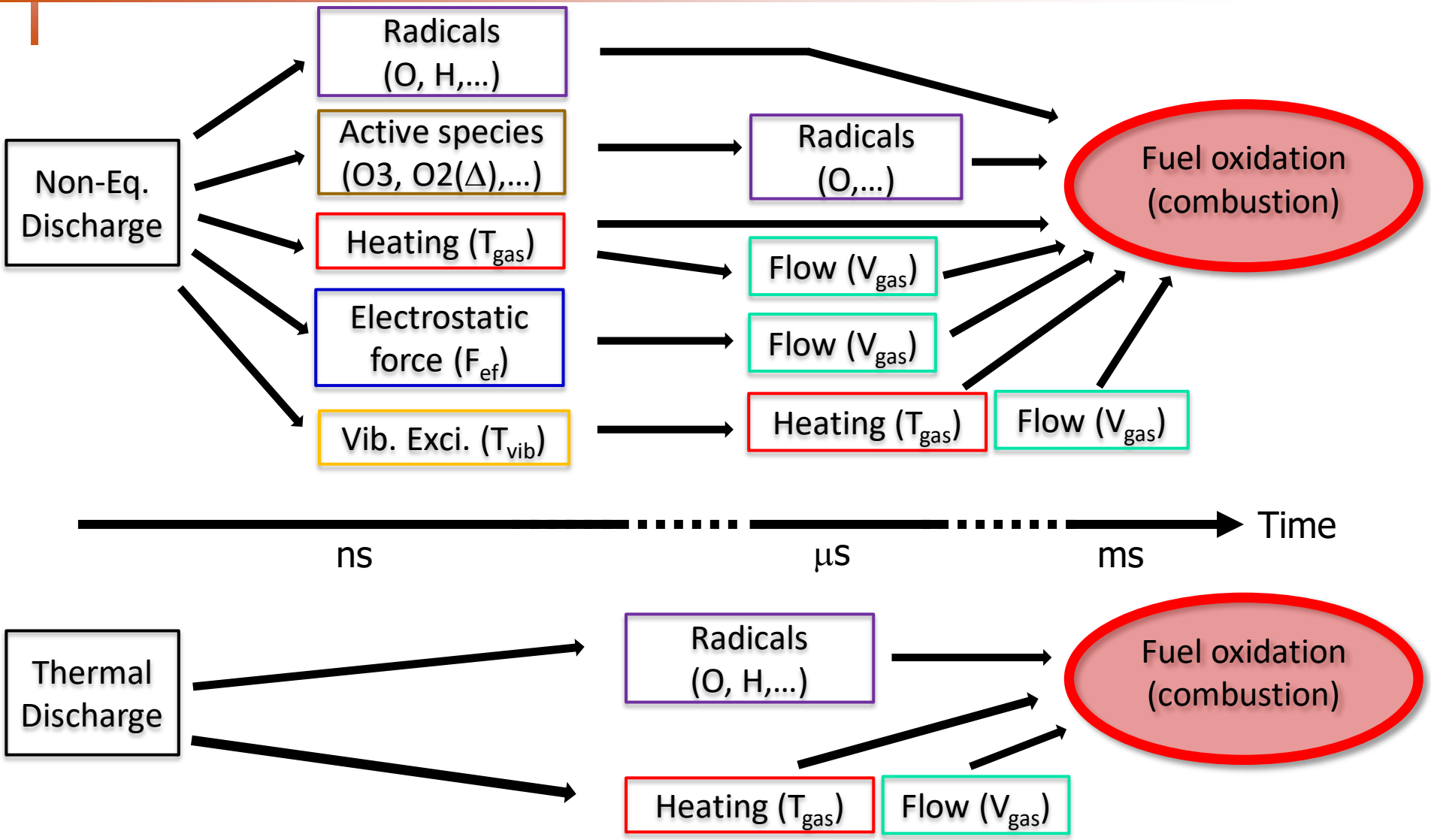

Adapted and extension of: Castela et al., Comb. & Flame 166, 133 (2016)

Non-equilibrium plasma model

- Species continuity

$$\frac{\partial n_k}{\partial t} + \vec{\nabla} \cdot \vec{f}_k = \dot{G}_k \qquad k = 1, \ldots, K_{\text{gas}} \; (k \neq k_{\text{back}})$$

- Ideal Gas Law

$$p = \sum_{k=1}^{K_{\text{gas}}} n_k k_B T_k$$

- Drift-Diffusion approximation with bulk convection

$$\vec{f}_k = n_k \vec{u}_k = n_k \left(\vec{u} + \vec{U}_k \right) = n_k \vec{u} + \vec{\Gamma}_k$$

- Poisson's equation

$$\vec{\nabla} \cdot \left(\varepsilon_r \vec{\nabla} \phi \right) = -\frac{\rho_c}{\varepsilon_0} \qquad \rho_c = e \sum_{k=1}^{K_{\text{gas}}} Z_k n_k$$

- Electron Energy Equation

$$\frac{\partial e_e}{\partial t} + \vec{\nabla} \cdot \left[(e_e + p_e) \vec{u}_e + \vec{q}_e \right] = S_e \qquad e_e \approx \frac{3}{2} k_B T_e n_e$$

$$S_e = \vec{j}_e \cdot \vec{E} - e \sum_{i=1}^{I_{\text{gas}}} \Delta E_i^e \dot{r}_i - \frac{3}{2} k_B n_e \left(\frac{2 m_e}{m_b} \right) \left(T_e - T_g \right) \bar{\nu}_e$$

Flow model

- Compressible Navier-Stokes eqn.

$$\frac{\partial \mathbf{U}}{\partial t} + \vec{\nabla} \cdot (\vec{\mathbf{F}} - \vec{\mathbf{G}}) = \mathbf{S}$$

State vector:

$$\mathbf{U} = \begin{bmatrix} \rho \\ \rho u \\ \rho v \\ \rho w \\ \rho E \end{bmatrix}$$

Flux vectors:

$$\vec{\mathbf{F}} = \begin{bmatrix} \rho\vec{v} \\ \rho\vec{v}u + p\hat{\imath} \\ \rho\vec{v}v + p\hat{\jmath} \\ \rho\vec{v}w + p\hat{k} \\ \rho\vec{v}H \end{bmatrix} \quad \vec{\mathbf{G}} = \begin{bmatrix} 0 \\ \tau_{xx}\hat{\imath} + \tau_{xy}\hat{\jmath} + \tau_{xz}\hat{k} \\ \tau_{yx}\hat{\imath} + \tau_{yy}\hat{\jmath} + \tau_{yz}\hat{k} \\ \tau_{zx}\hat{\imath} + \tau_{zy}\hat{\jmath} + \tau_{zz}\hat{k} \\ \bar{\bar{\tau}}.\vec{v} - \vec{q} \end{bmatrix}$$

Eqn. of State:

$$p = \rho RT$$

$$E = \int c_p dT + \frac{V^2}{2} - \frac{p}{\rho}$$

Source vector:

$$\mathbf{S} = \begin{bmatrix} 0 \\ F_{ef,x} \\ F_{ef,y} \\ F_{ef,z} \\ s_t + \vec{F}_{ef}.\vec{u} \end{bmatrix}$$

Electrostatic forcing

$$\vec{F}_{ef} = \rho_c \vec{E}$$

Gas heating

$$S_t = \xi\, \vec{j}_i \cdot \vec{E} - e \sum_{i=1}^{I_{\text{gas}}} \Delta E_i^h \dot{r}_i - \frac{3}{2} k_B n_e \left(\frac{2m_e}{m_b}\right)(T_e - T_g)\bar{\nu}_e$$

Breden and Raja, AIAA J. 50, 647 (2012)

Additional physics representation

- Surface charge trapping on dielectric surfaces

$$\frac{\partial \rho_s}{\partial t} = \sum_{k=1}^{K_{\text{gas}}} \vec{j}_k \cdot \hat{n}_s$$

- Chemistry
  - Air
  - Methane + Air

26 Species :

E, O, N_2 , O_2 , H , N_2^+ , O_2^+ , N_4^+ , O_4^+ , $O_2^+N_2$, O_2^- , O^- , O_2(a1) , O_2(b1) , O_2* , N_2(A) , N_2(B) , N_2C , N_2(a1), CH_4 , CH_3 , CH_2 , CH_4^+, CH_3^+ , CH_2^- , H^-

85 Reactions :

1) electron impact excitation (rot,vib,el), dissociation, ionization, 2) excited species quenching (fast gas heating), 3) ion-neutral (chx,…), 4) neutral-neutral

[Not included: Ozone chem., V-T transfer, fuel oxidation kinetics]

- Photoionization

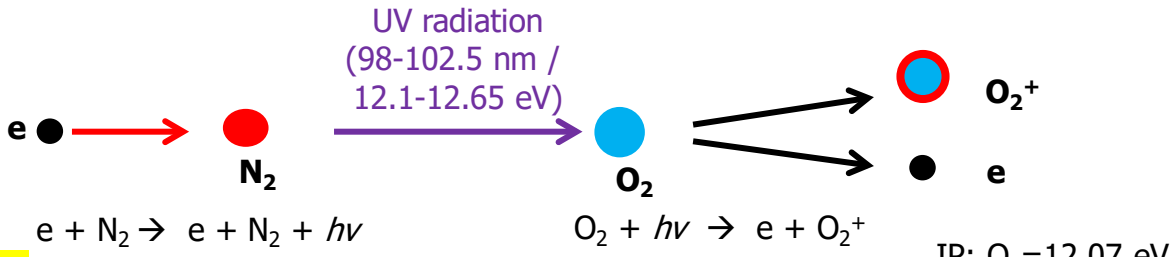

IP: O_2=12.07 eV

Breden et al., J. Appl. Phys. 114, 083302 (2013)

Computational issues

- Computational difficulties are primarily dictated by spatial and temporal stiffness

Temporal Stiffness

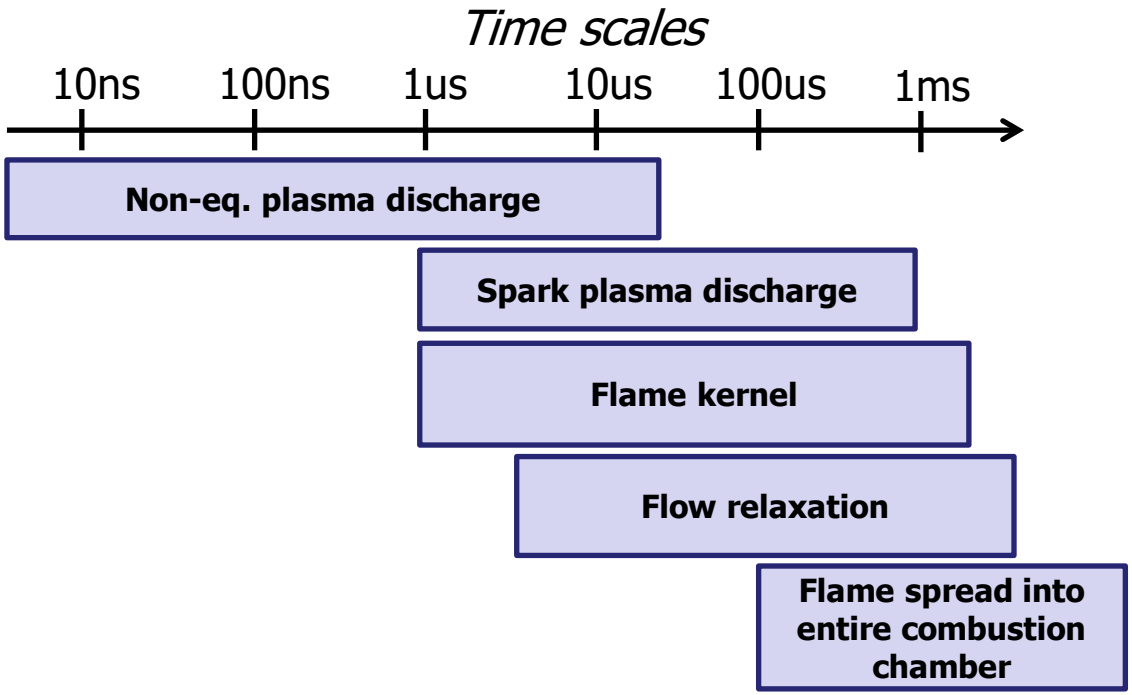

Spatial Stiffness

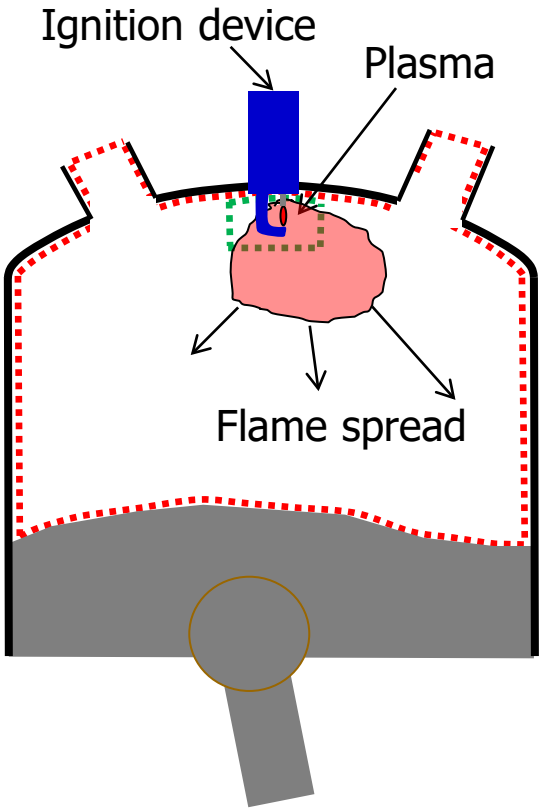

Computational approach (Alleviation of temporal stiffness)

- Physics-dependent TIME-STEP SKIPPING:

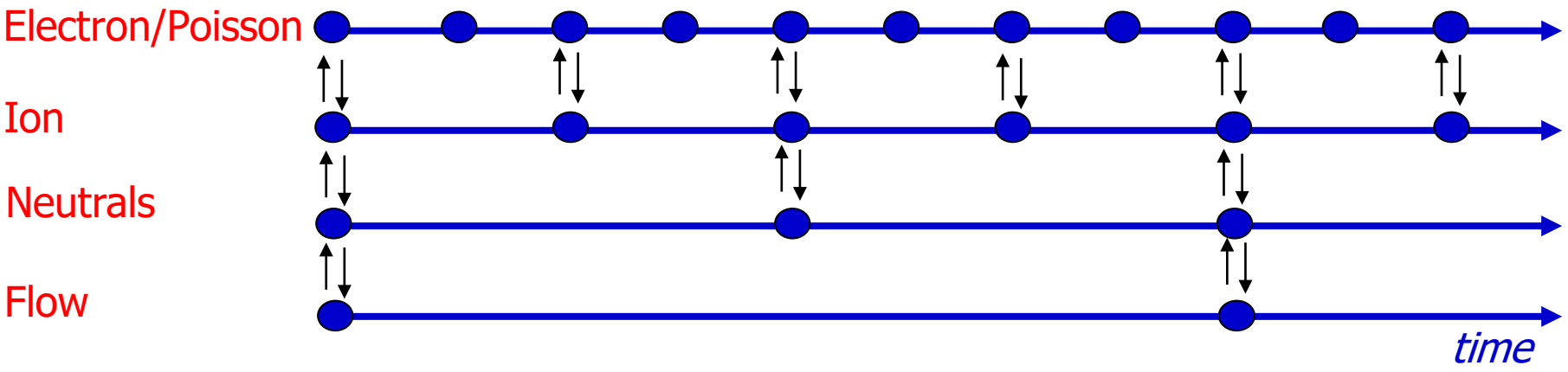

- Physics-dependent TIME-STEP MULTIPLICATION
  - for steady/periodic steady problems

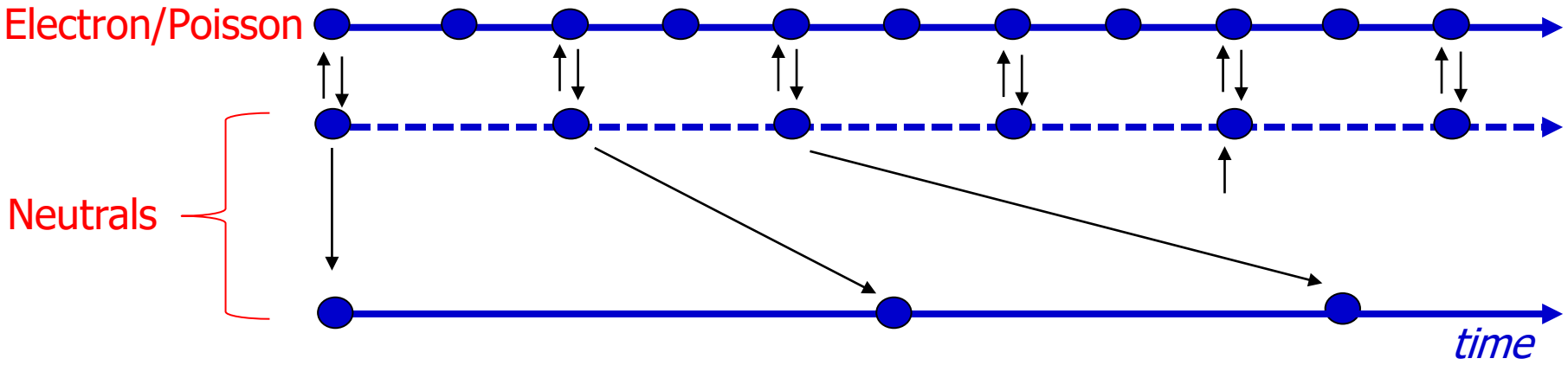

Computational approach (Alleviation of spatial stiffness)

- Subdomain-dependent equation selection
- Unstructured mesh

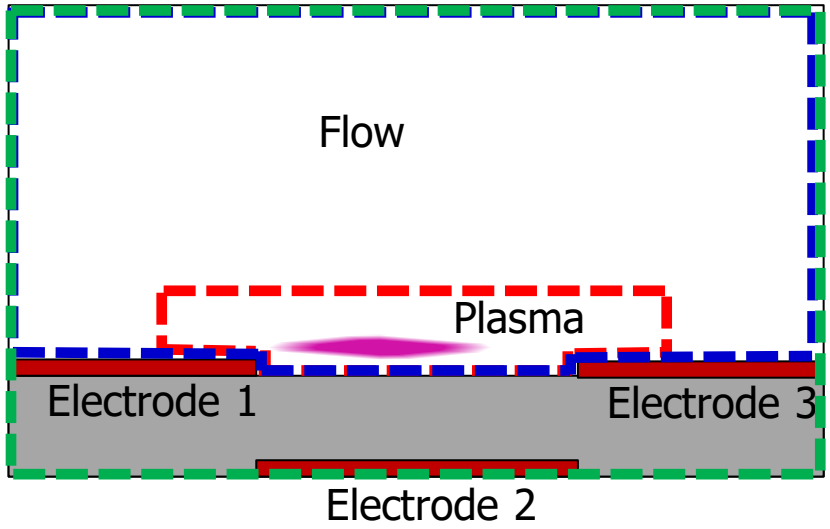

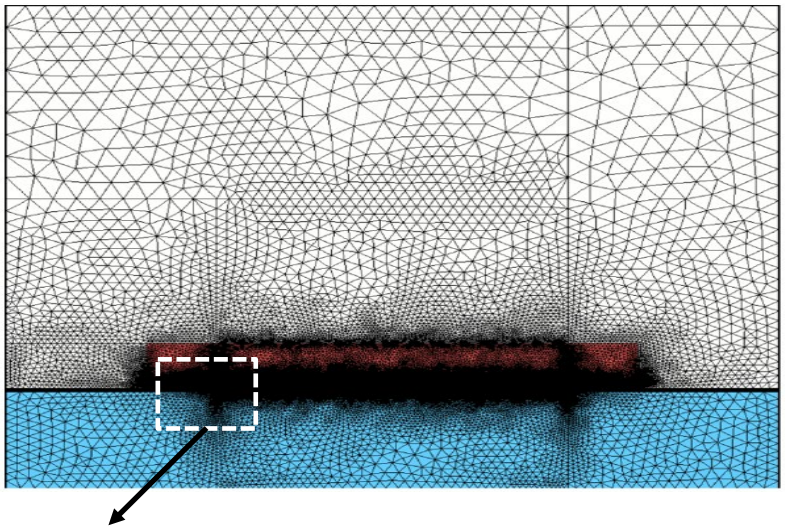

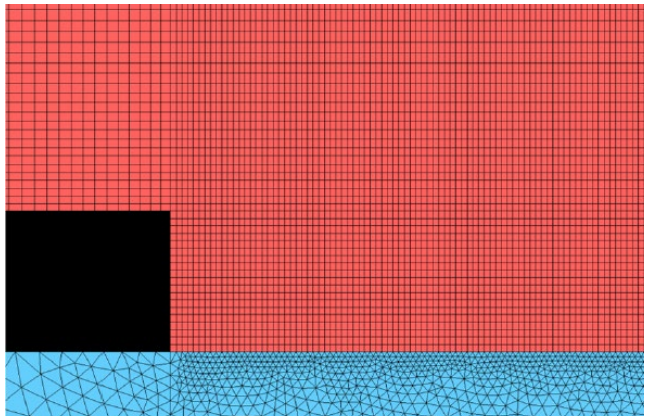

Example: Nanosecond Pulsed (NSP) Coaxial and Corona Igniter in Combustible Mixture

Breden, Raja, Idicheria, Najt, and Mahadevan, J. Appl. Phys. 114, 083302 (2013)

Coaxial electrode NSP plasma simulation

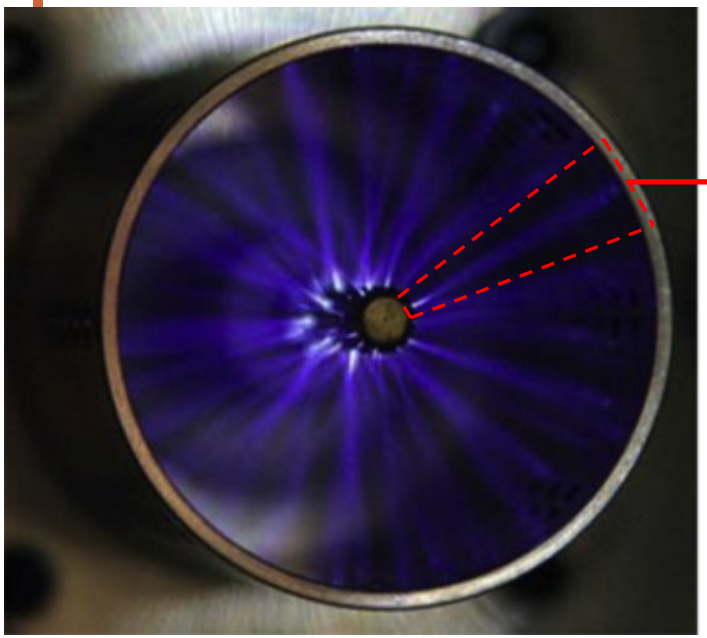

M. Gundersen, Univ. Southern California

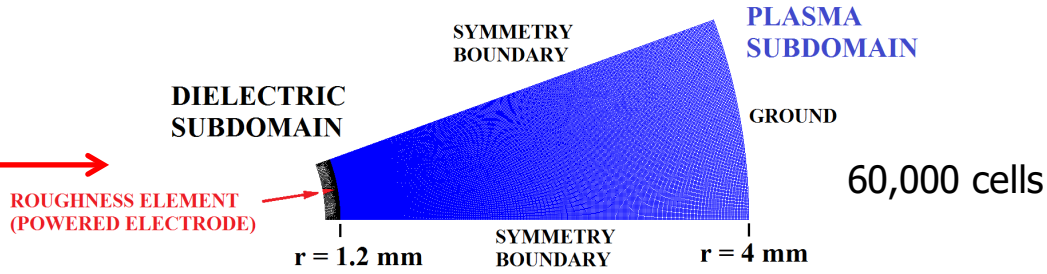

60,000 cells

- Simulation conditions:
  - 10 atmospheres
  - 700 K fixed gas temperature
  - 40 kV applied voltage (E/n ~ 143 Td)
  - lean A/F ratio (40:1 air/methane)

- Simulation domain : sector of annular domain
  - 20 deg. sector angle
  - Characteristic size for single streamer propagation
  - Roughness element on inner electrode to pin location of streamer

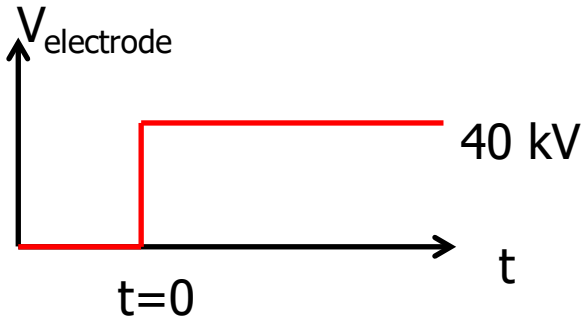

Time evolution of electron density and temperature for coaxial electrode NSP

Conditions: P=10 atm, T_{gas}=700 K, 40 kV, 40:1 A/F ratio (lean)

Electron density transient

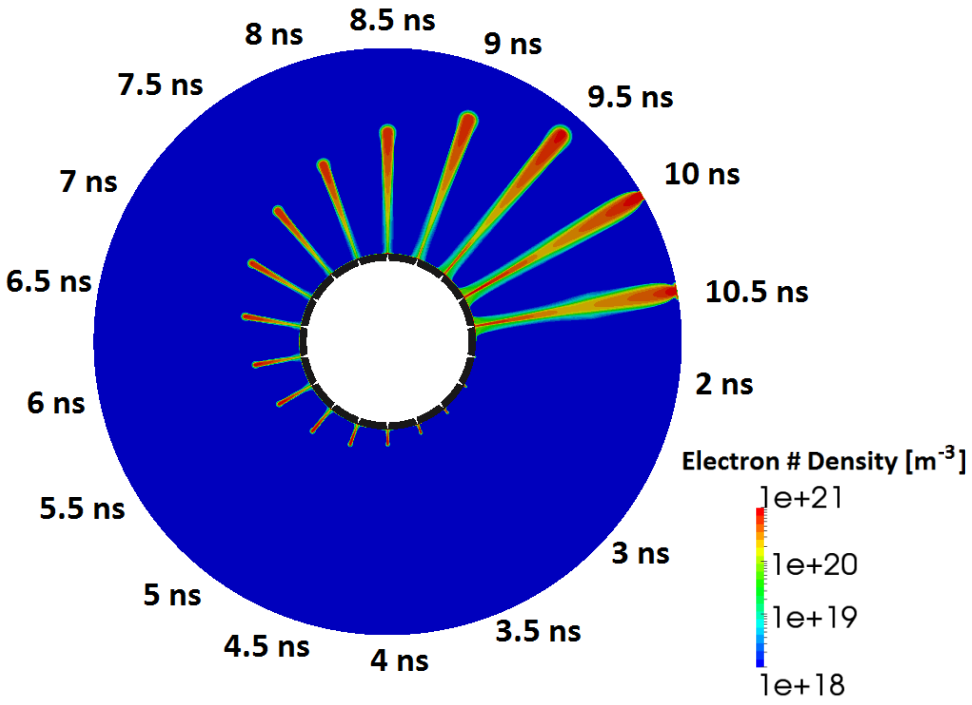

Electron temperature transient

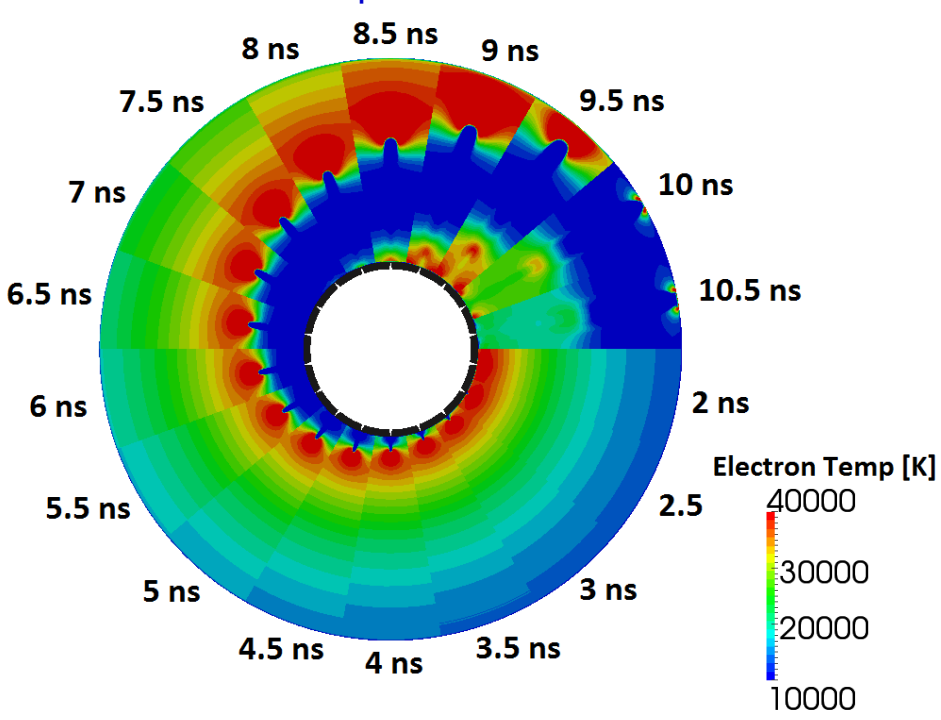

- 2 ns induction time (defined: time to reach threshold of 10^{19} m^{-3})
- Streamers bridge electrode gap in about 10 ns
- N_e(peak)~ 10^{21} m^{-3} , T_e(head) ~4 eV, T_e(body) ~1 eV
- Secondary streamer (source of luminosity?)

Time evolution of radical densities and for coaxial electrode NSP

Conditions: P=10 atm, T_{gas}=700 K, 40 kV, 40:1 A/F ratio (lean)

O radical density transient

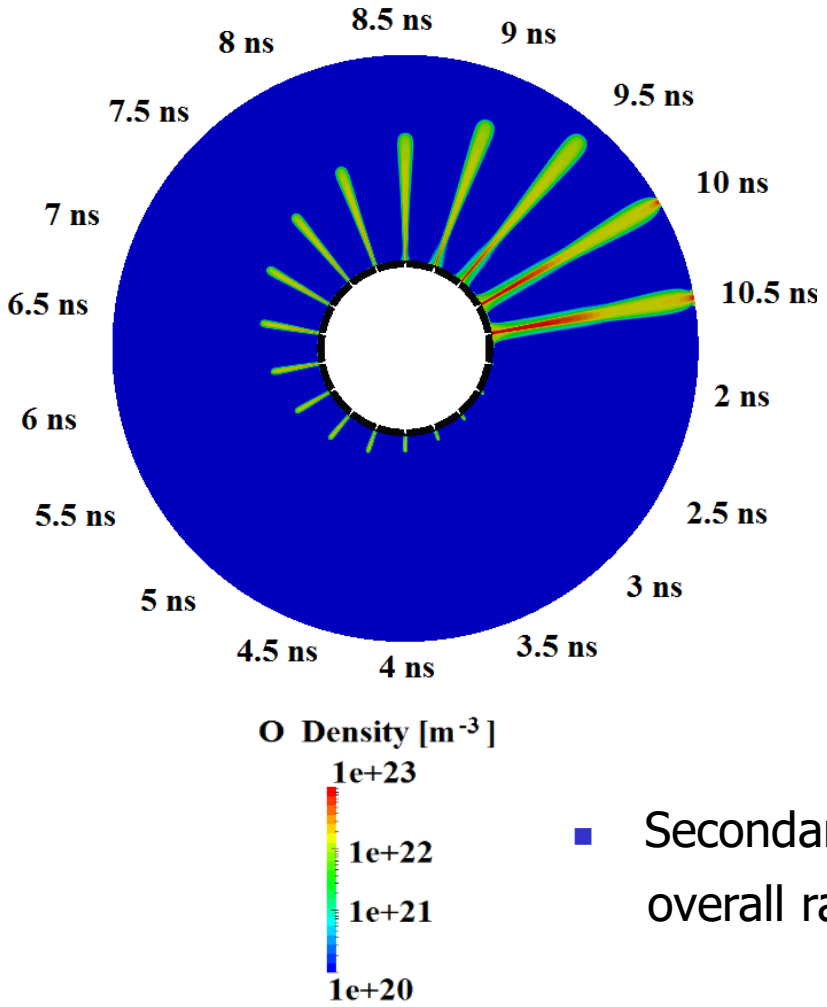

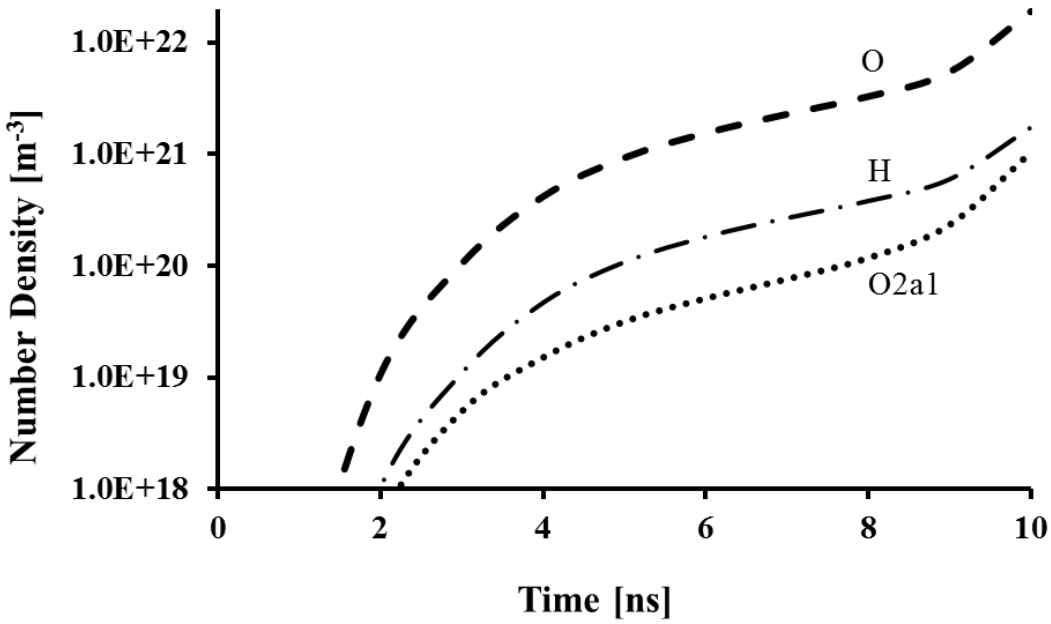

- Secondary streamer has significant impact on overall radical yield

Corona igniter

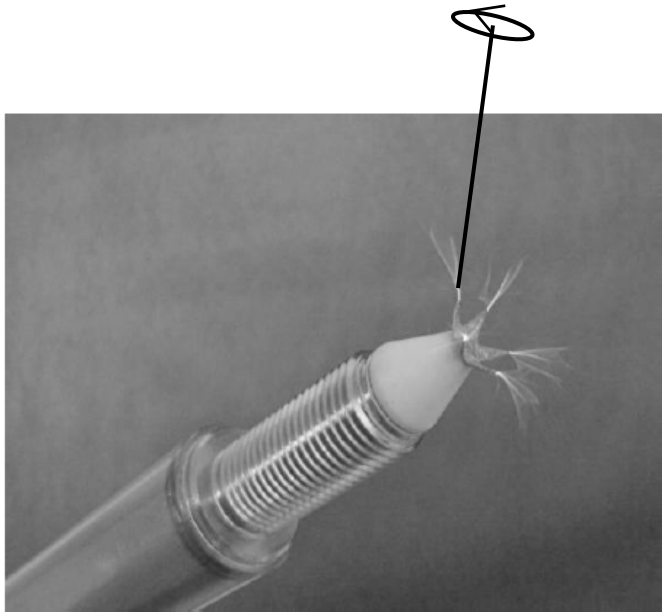

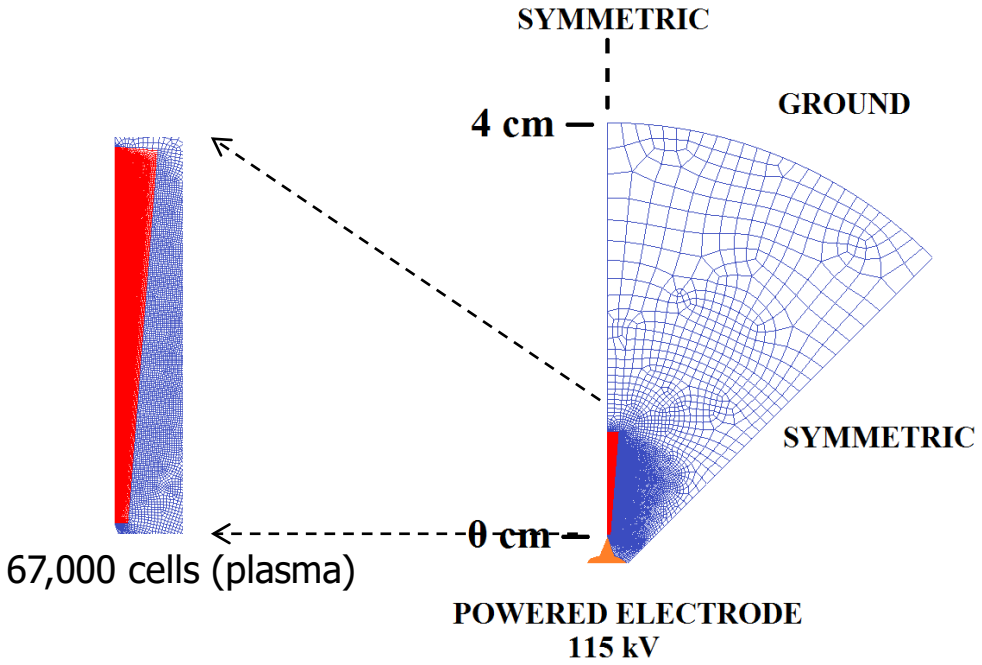

- Simulation conditions:
  - 10 atmospheres
  - 700 K fixed gas temperature
  - 115 kV applied voltage
  - lean A/F ratio (40:1 air/methane)

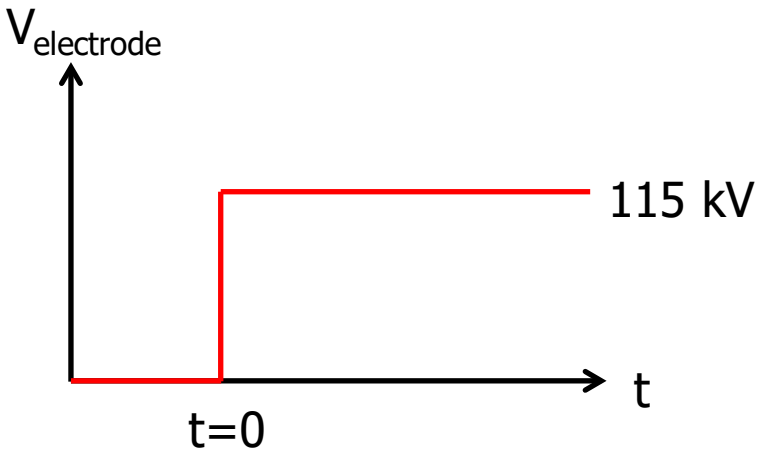

Transient evolution of electron density

Conditions: P=10 atm, T_{gas}=700 K, 115 kV, 40:1 A/F ratio (lean)

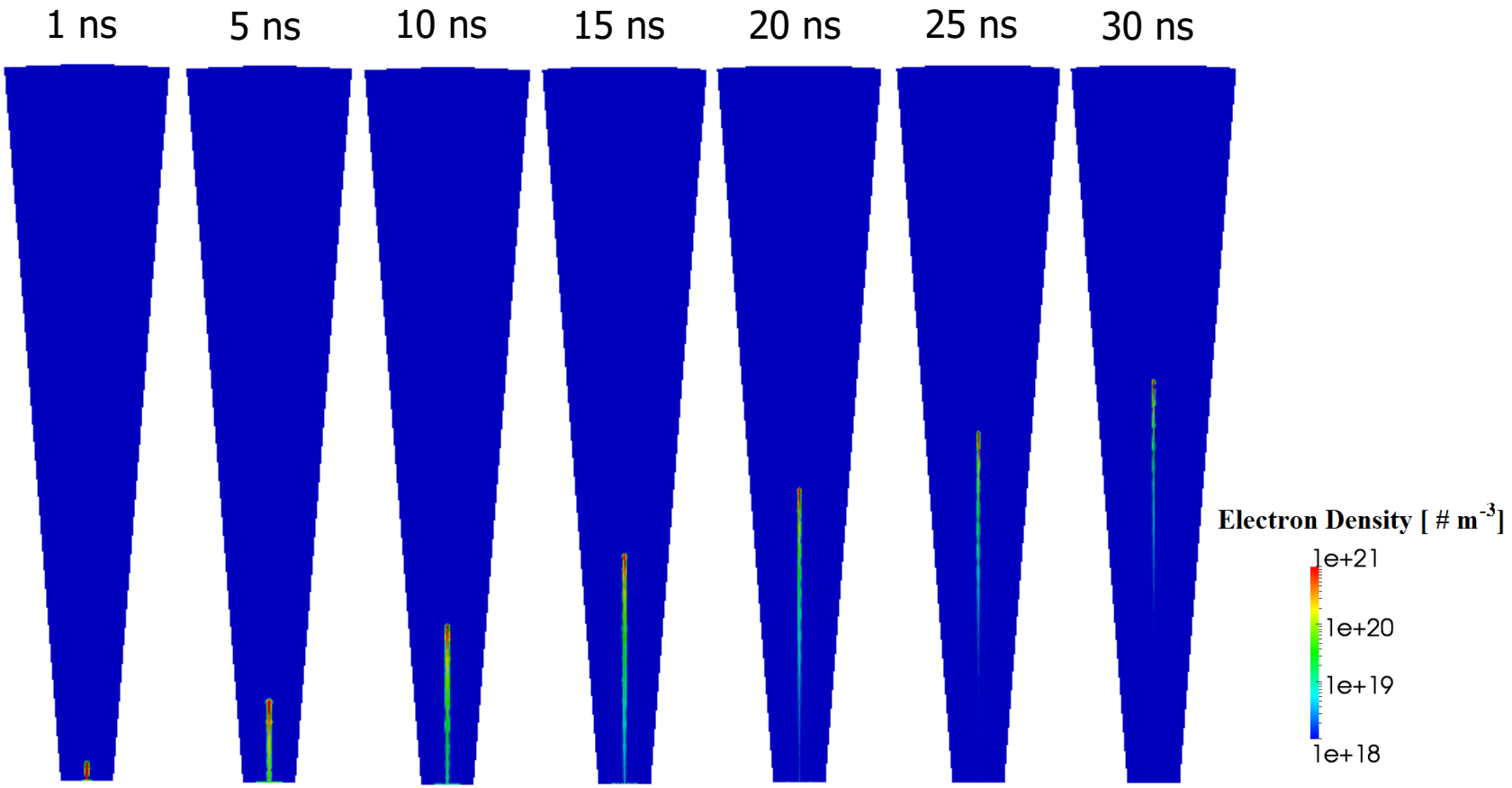

- Peak electron densities in streamer head (~10^{21} m^{-3})
- Electron attachment in body

Comparison of species yields for Coaxial and Corona electrode geometries

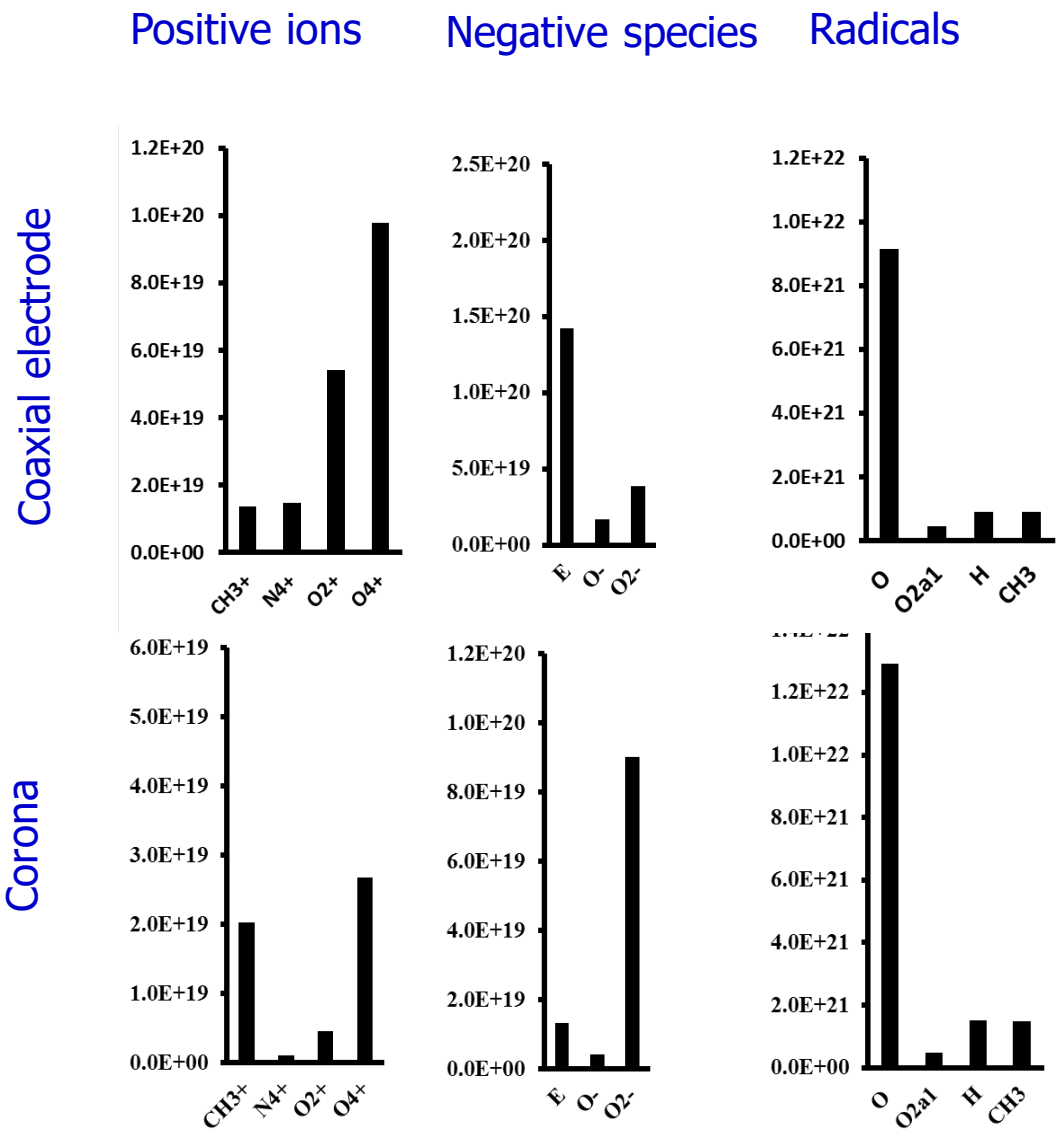

Example: Nanosecond Pulsed (NSP) in Spark-plug configuration

Karpatne, Breden, and Raja., SAE Technical Paper (2017)

Example: Nanosecond pulsed in pin-to-pin configuration

- Problem Specifications
  - 2-D Axisymmetric Spark Plug, Spark gap = 0.7 mm
  - Electrode dia. = 0.25 mm
  - Applied cathode voltage (kV) = -11 kV to -18 kV
  - Pressure ~ 3 atm.
  - Temperature = 300 K
  - Air chemistry
  - Quenching surface chemistry included

- Numerical Specifications
  - # Cells ~ 32,000
  - dt ~ 1e-14 s
  - Parallel (**16 procs**), **t ~ 30 hrs**
  - Final time ~ 1.5 ns

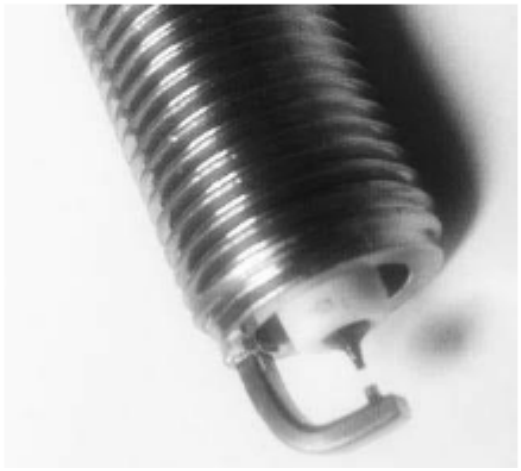

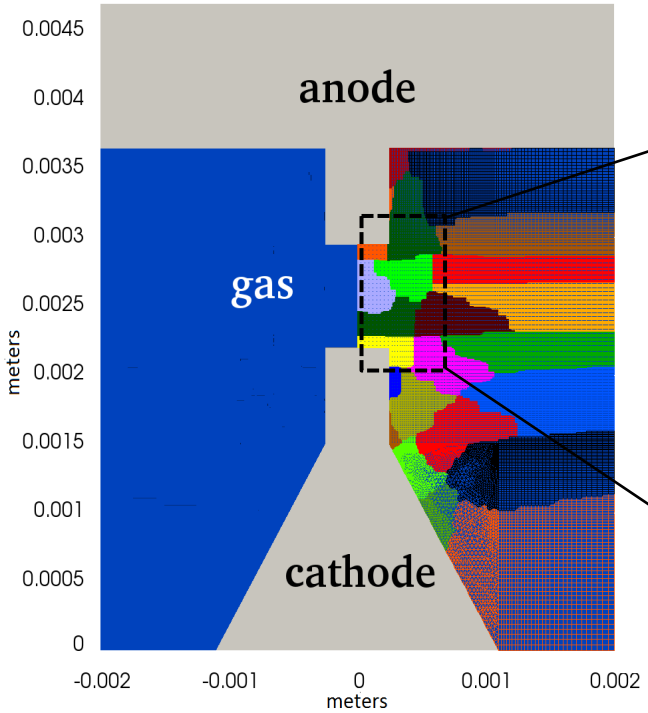

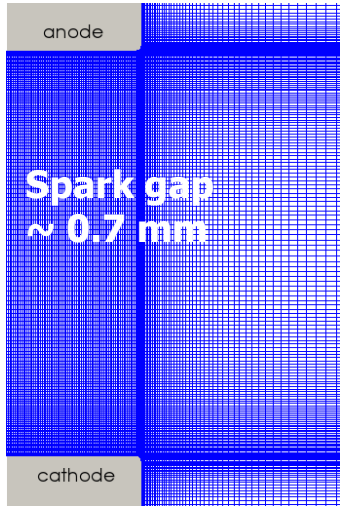

Plasma structure in the spark gap

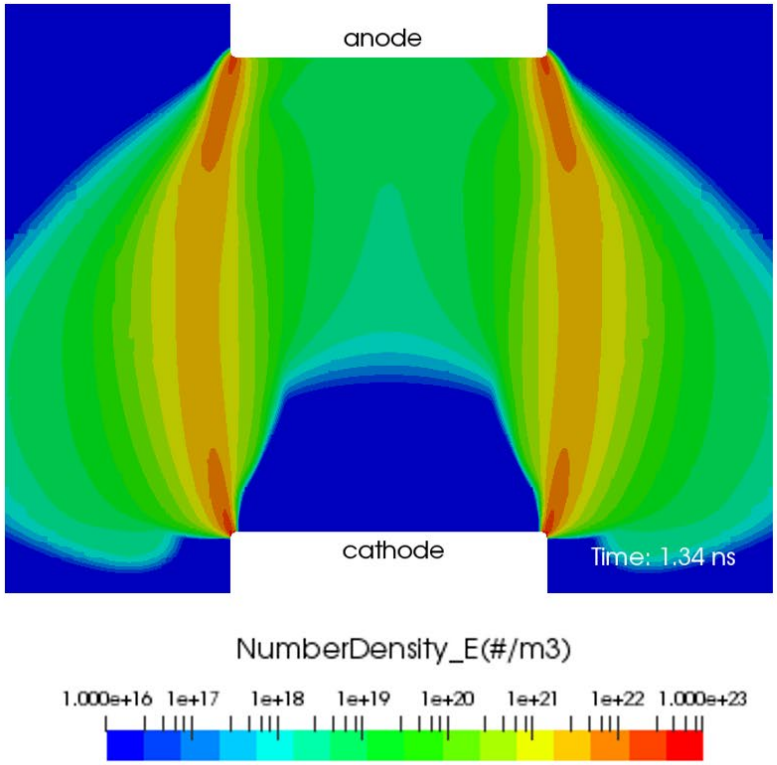

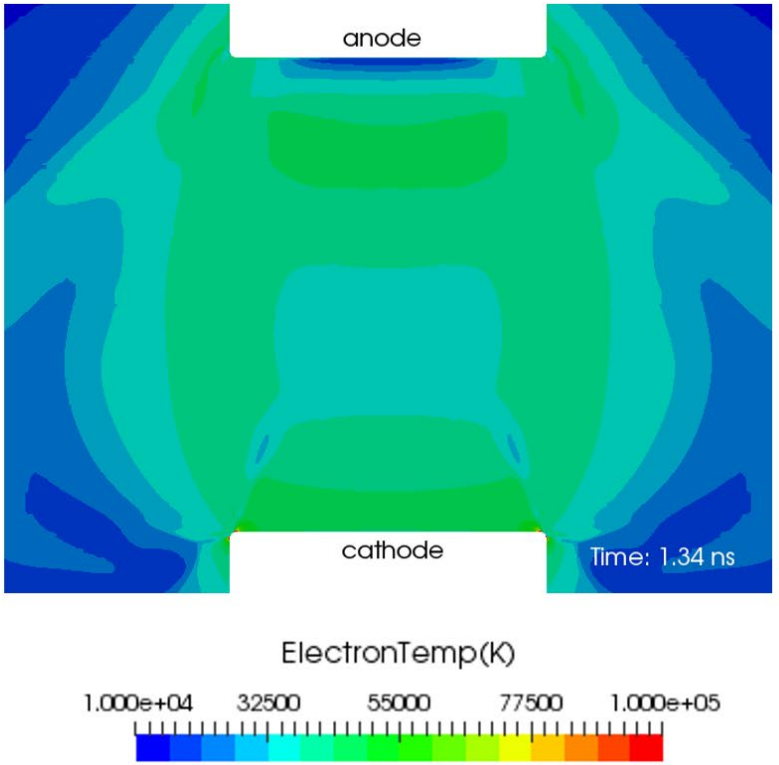

- Streamers originate at the E-field intensified regions of the electrode tips.
- Anode-directed (negative) streamer first emerges at 0.25 ns
- E-field distortion of negative streamer causes a positive streamer at 0.7 ns
- Streamers merge after about 0.9 ns forming a conductive pathway
- Eventually leads to large current flows (secondary breakdown)

Charged species evolution

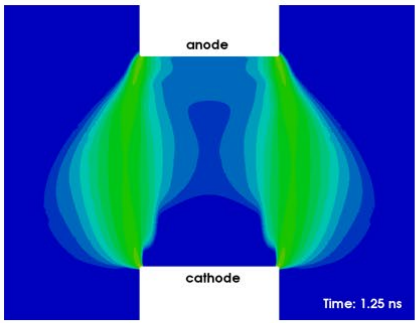

N4+

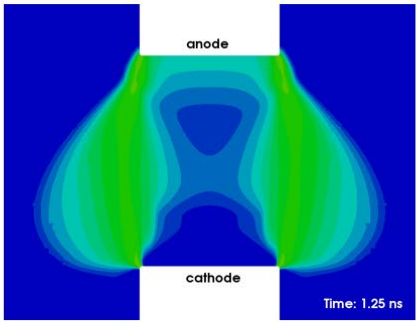

O2+

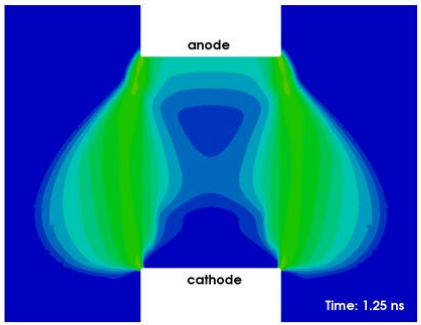

O4+

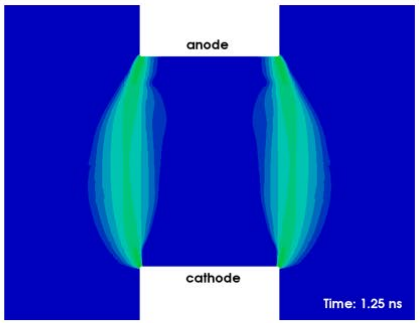

N2+

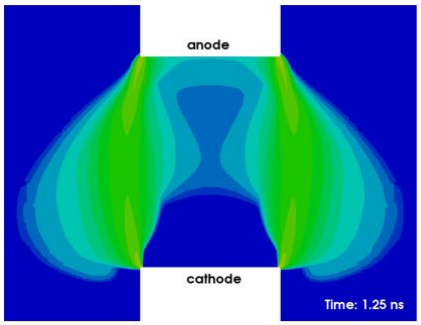

Electrons

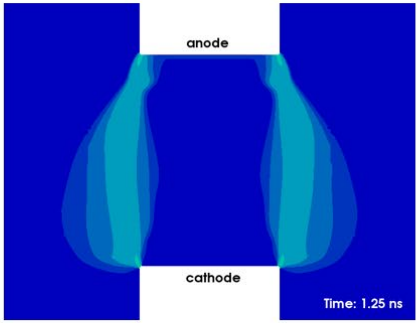

O2-

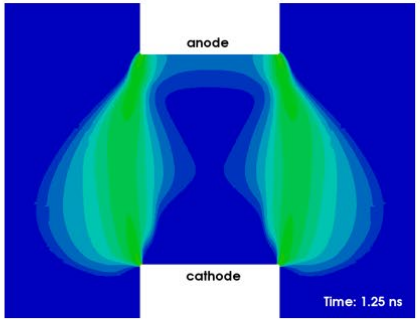

O-

Number Density (#/m^3)

Nitrogen and oxygen radical/exited species

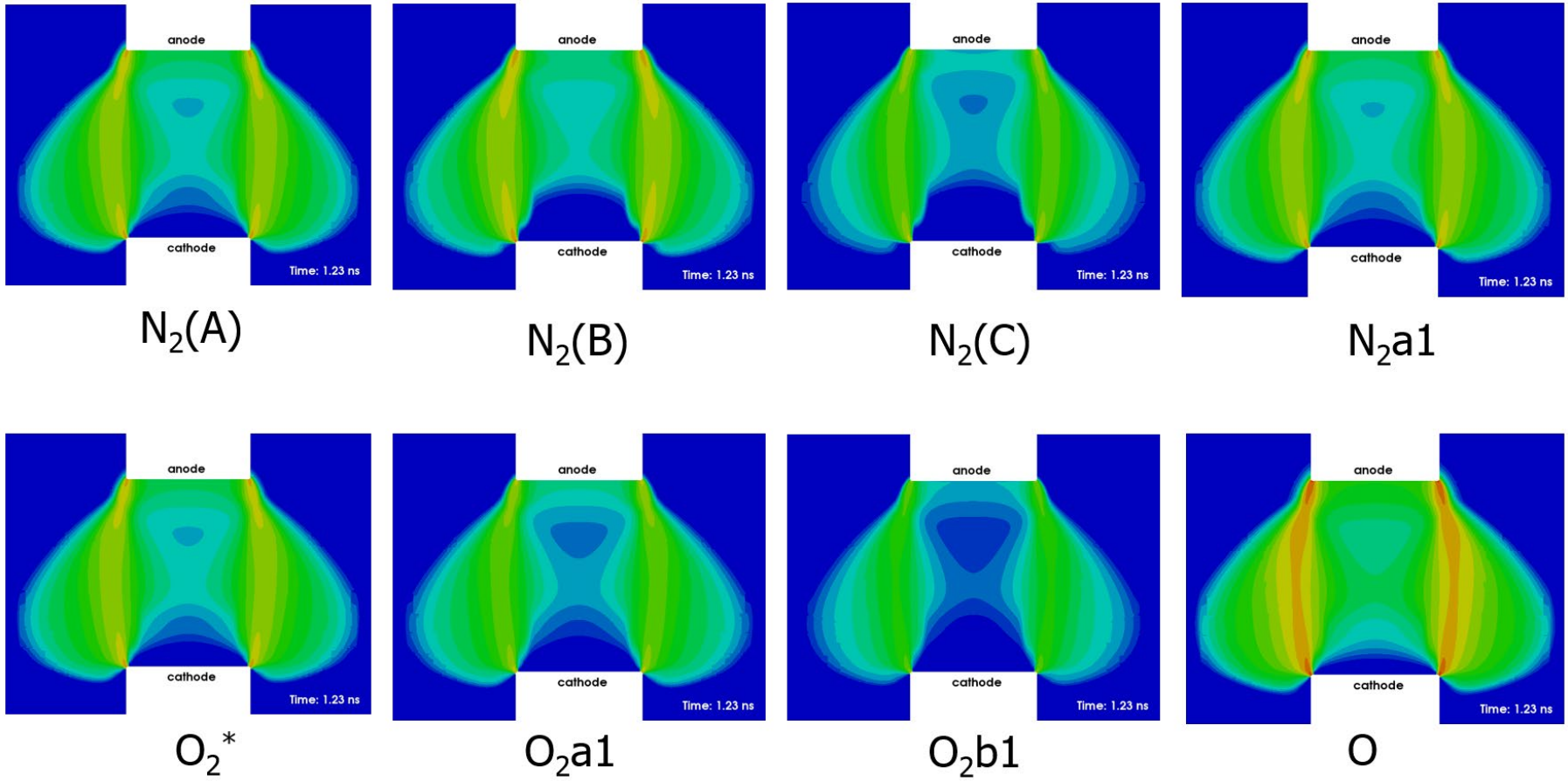

Fast gas heating and early flow response (~1.5 ns)

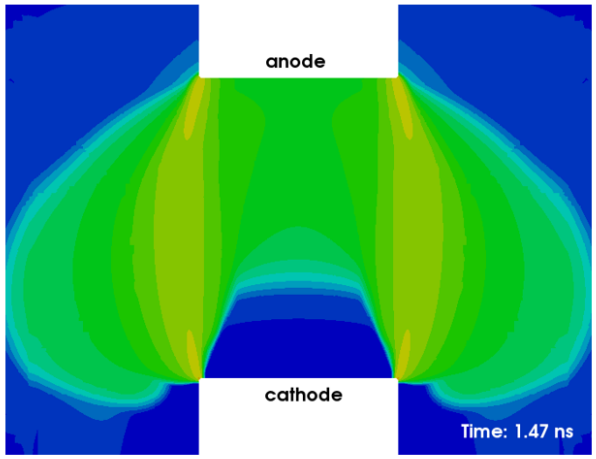

Elastic Collision Source (W/m^3)

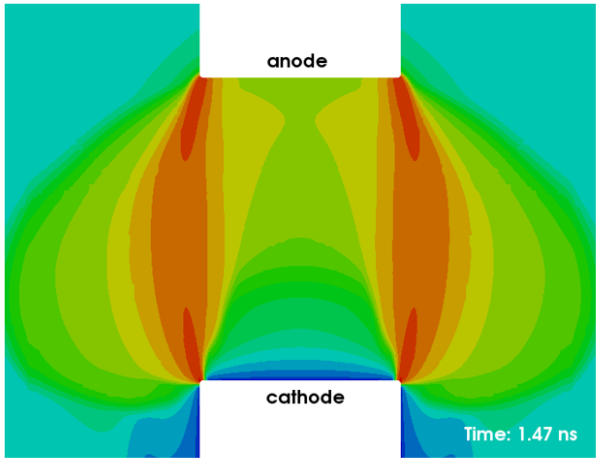

Inelastic Collision Source (W/m^3)

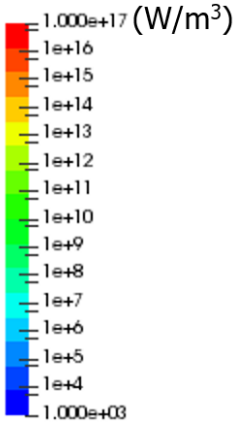

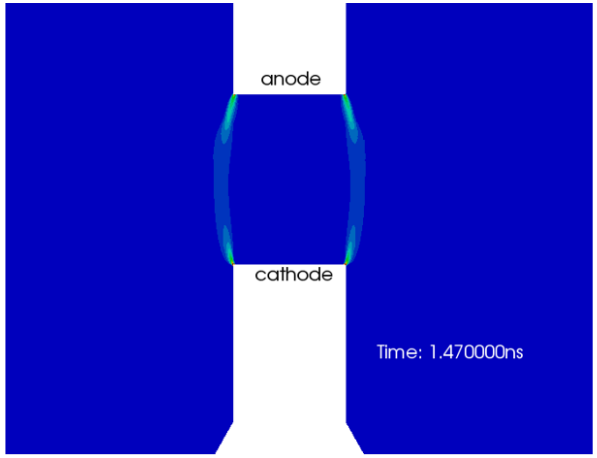

Temperature (K)

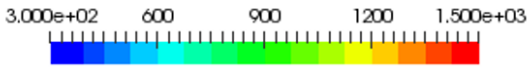

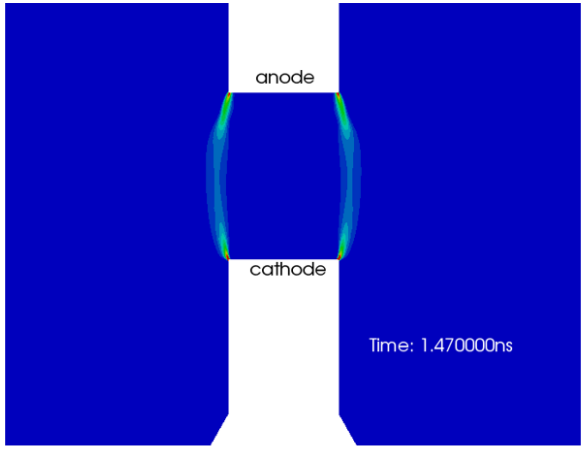

Pressure (Pa)

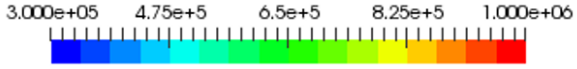

Flow response (longer time scale ~1 μs)

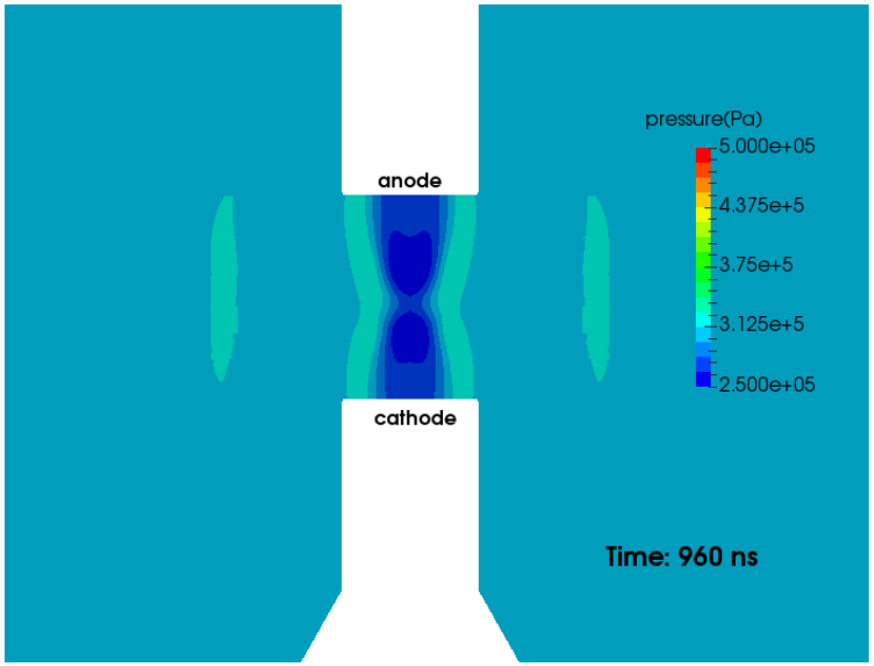

Pressure (Pa)

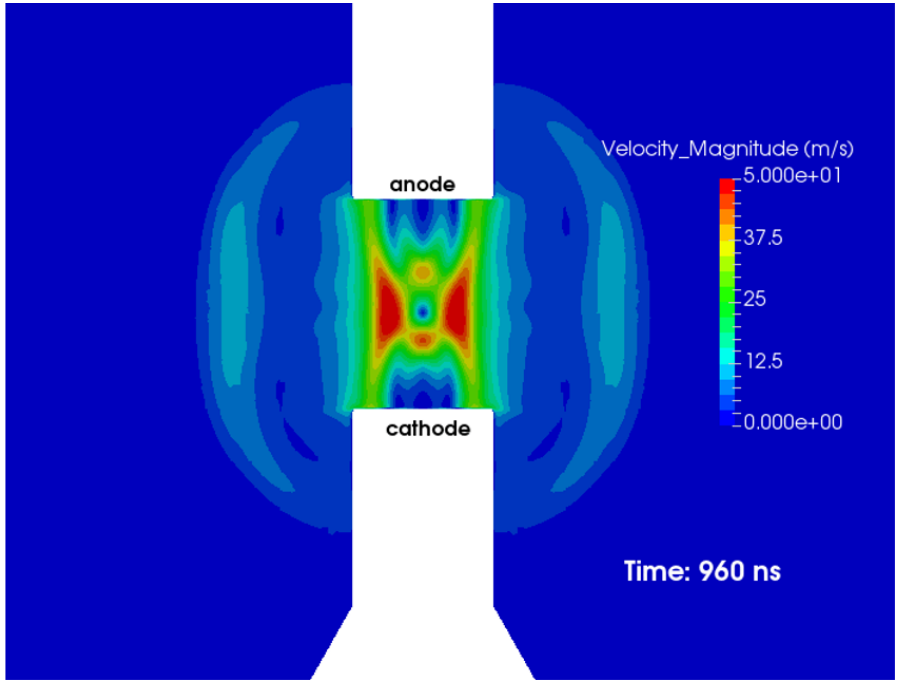

Flow velocity (m/s)

- Plasma heating active up to 1.3 ns.
- Gas dynamic response to heating shown here from t = 1 ns to t =1000 ns.
- Inward and outward propagating shock relief (wave vel. ~1000 m/s)
- Induced flow velocities (~ 50 m/s)

Time evolution of electrode currents

- Streamer formation from 0-0.5ns, spark gap is highly **resistive** and no current flows through it
- At ~0.5 ns streamer root connects with cathode with observed current spike
- At 0.9 seconds primary cathode and anode streamers merge
- After 1 ns, channel conductivity increases dramatically indicating onset of a secondary breakdown and transition to arc
- The current spikes when streamers merge corresponding to spikes in ion flux to surfaces

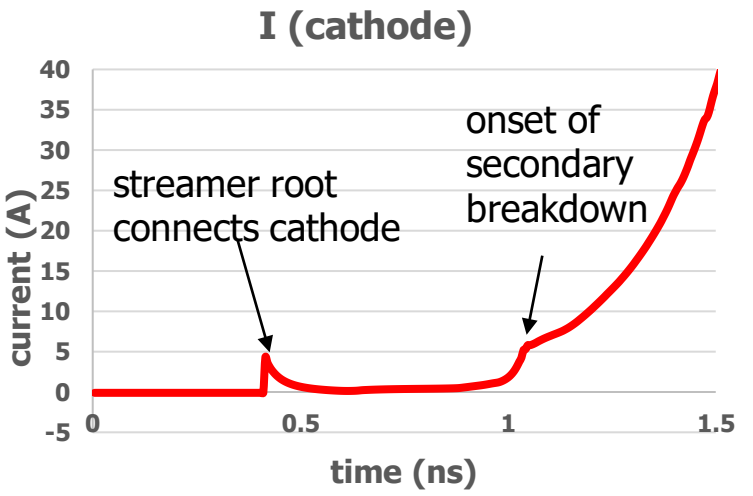

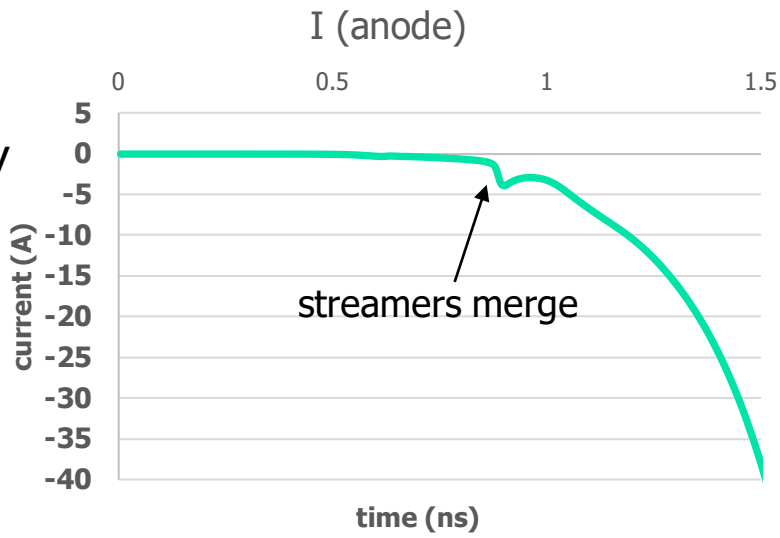

Species flux and impact energies (cathode)

- Total Cathode wall flux and surface impact energies are shown at 1.5ns.
- Significant ion flux is observed at the cathode corner (~ 10^{28} #/s)
- Max impact energy is **~ 300 eV**
- Typical sputter energy threshold ~ **30 eV** for most metals

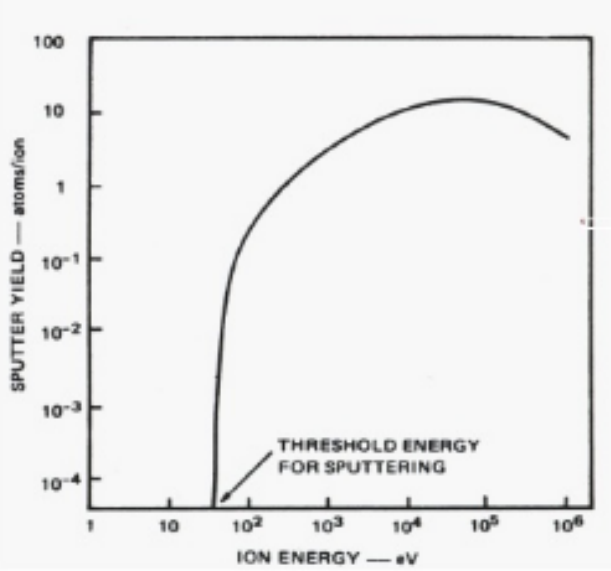

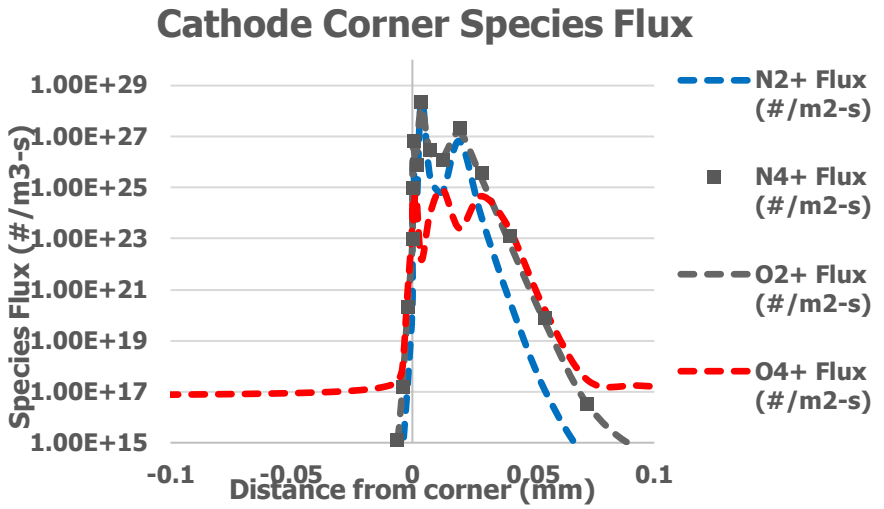

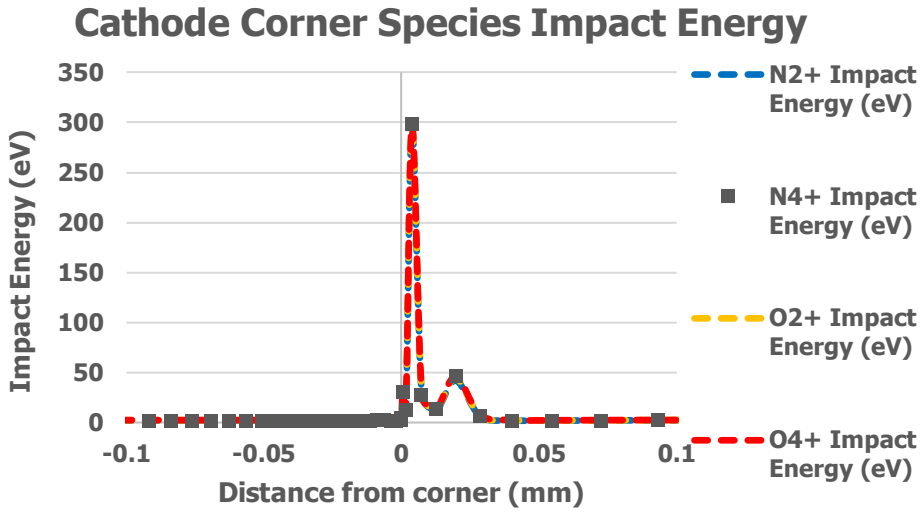

Species flux and impact energies (anode)

- Anode corner wall flux and surface impact energies are shown at 1.5ns (after channel has formed)
- Mostly electrons, small amount of O_2^- ions.
- Max impact energy is **~ 12 eV** for O_2^- and O^- ions and **~ 0.1 eV** for electrons
- Expect minimal damage on anode corner compared to cathode

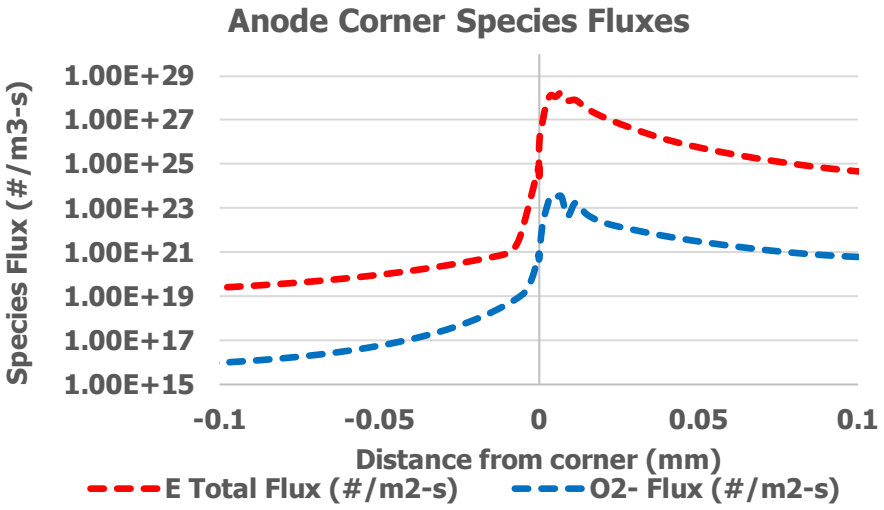

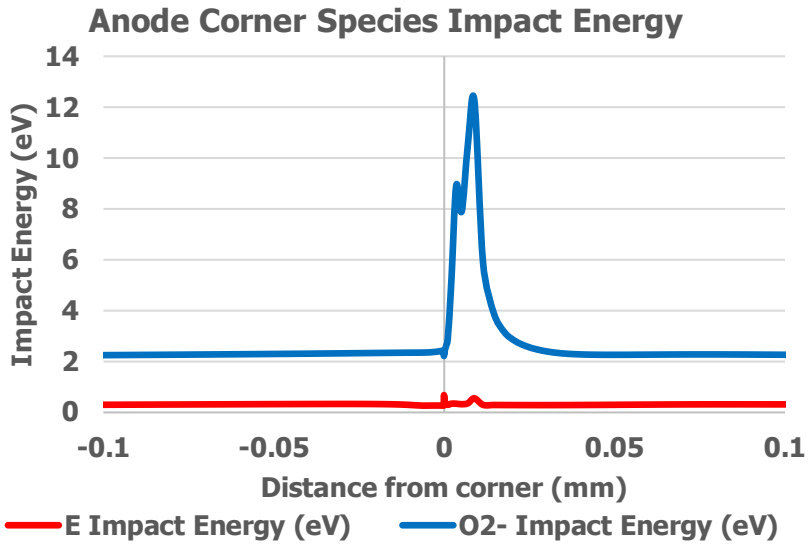

Example: Modeling of Thermal Arc Interaction with a Cross Flow

Breden, Mahadevan, and Raja., SAE Technical Paper (2016)

Arc model

- Compressible Navier-Stokes eqn.

$$\frac{\partial \mathbf{U}}{\partial t} + \vec{\nabla} \cdot (\vec{\mathbf{F}} - \vec{\mathbf{G}}) = \mathbf{S}$$

State vector:

$$\mathbf{U} = \begin{bmatrix} \rho \\ \rho u \\ \rho v \\ \rho w \\ \rho E \end{bmatrix}$$

Flux vectors:

$$\vec{\mathbf{F}} = \begin{bmatrix} \rho\vec{v} \\ \rho\vec{v}u + p\hat{\imath} \\ \rho\vec{v}v + p\hat{\jmath} \\ \rho\vec{v}w + p\hat{k} \\ \rho\vec{v}H \end{bmatrix} \quad \vec{\mathbf{G}} = \begin{bmatrix} 0 \\ \tau_{xx}\hat{\imath} + \tau_{xy}\hat{\jmath} + \tau_{xz}\hat{k} \\ \tau_{yx}\hat{\imath} + \tau_{yy}\hat{\jmath} + \tau_{yz}\hat{k} \\ \tau_{zx}\hat{\imath} + \tau_{zy}\hat{\jmath} + \tau_{zz}\hat{k} \\ \bar{\bar{\tau}}.\vec{v} - \vec{q} \end{bmatrix}$$

Eqn. of State:

$$p = \rho RT$$

$$E = \int c_p dT + \frac{V^2}{2} - \frac{p}{\rho}$$

Source vector:

$$\mathbf{S} = \begin{bmatrix} 0 \\ J_y B_z - J_z B_y + \rho g_x \\ J_z B_x - J_x B_z + \rho g_y \\ J_x B_y - J_y B_x + \rho g_z \\ \vec{J}.\vec{E} - \dot{Q}_{rad} \end{bmatrix}$$

EM coupling:

$$\vec{\nabla}.\vec{J} = 0$$

$$\vec{J} = \sigma\vec{E}$$

Geometry and configuration for spark-plug arc modeling problem

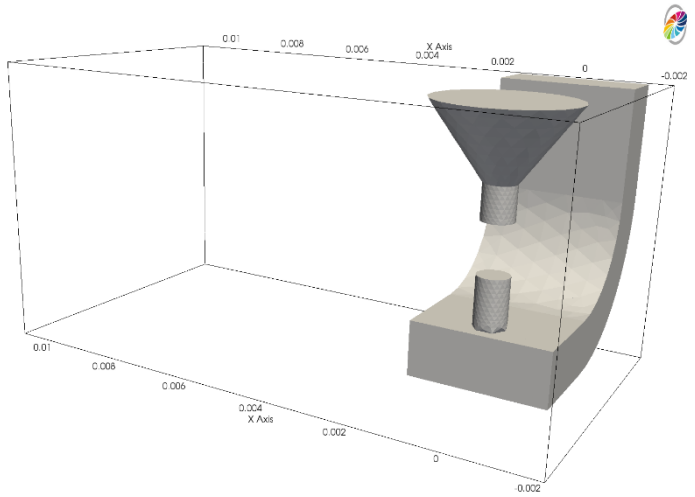

- Geometry : 1.1 mm gap sparkplug
  - 3-D 150K and 300K tetrahedral meshes
- Flow Environment
  - Mixture : Air
  - Temperature : 300 K
  - Pressure : 100-1000 kPa
  - Flow : 0-8 m/s

Circuit : Coil A (-50 mA)

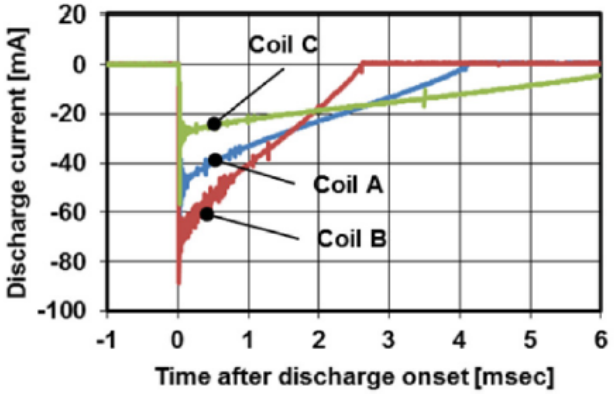

Shiraishi etal, SAE Intl. J. Engines, 9 (2016).

Key experimental observations

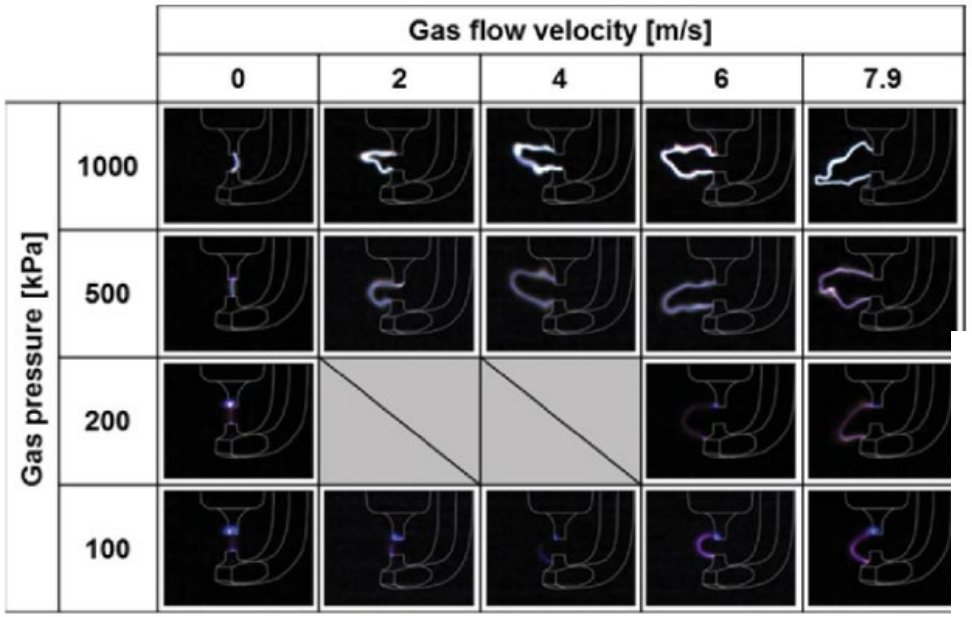

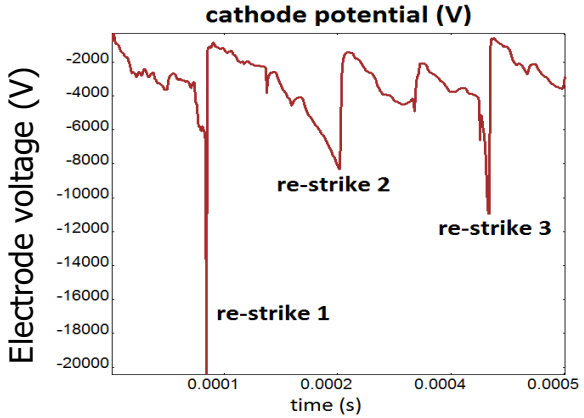

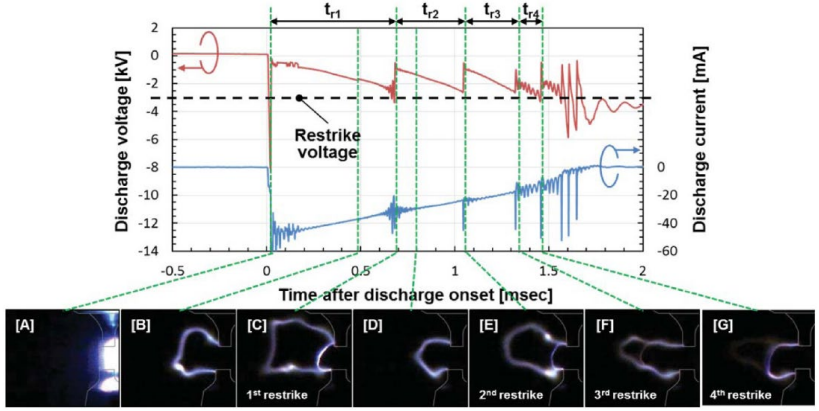

- Arc stretch due to cross flow (helps increase ignition kernel size)
- Arc encounters repeated restrike
- Arc structure and hence the ignition kernel properties are strong function of flow and pressure environment

Shiraishi etal, SAE Intl. J. Engines, 9 (2016).

Pressure = 100 kPa, Cross flow velocity = 4 m/s

- First re-strike event at 0.7 ms
- Re-strike voltage -2.75 kV

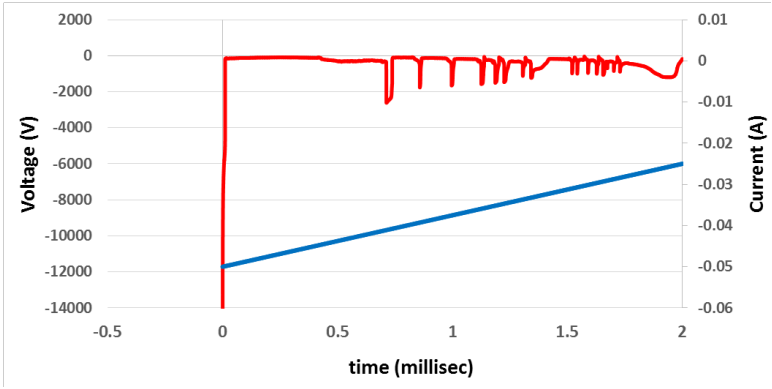

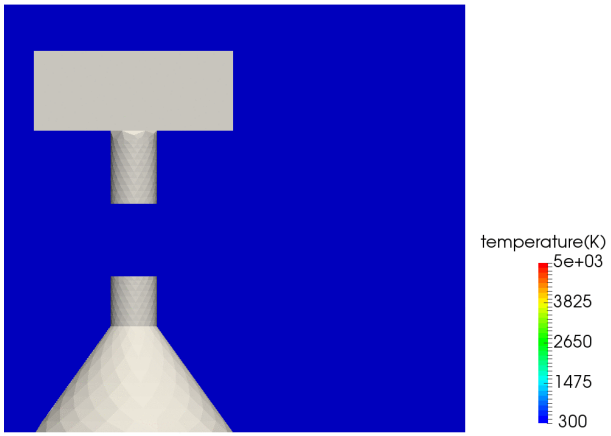

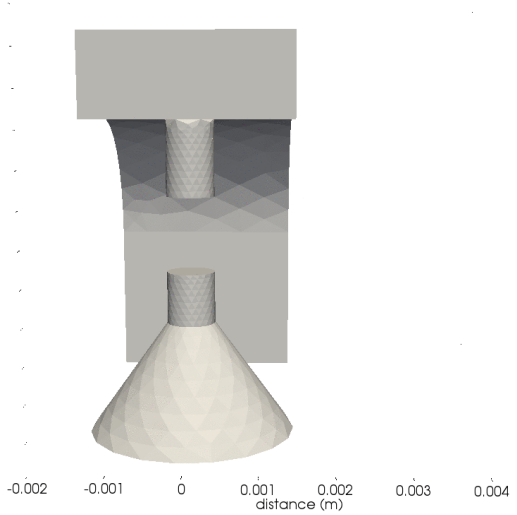

- Arc stretch due to cross flow improves ignition kernel size and hence ignition characteristics

Pressure = 100 kPa, Cross flow velocity = 8 m/s

- First re-strike event at 0.5 ms
- Re-strike voltage -4 kV

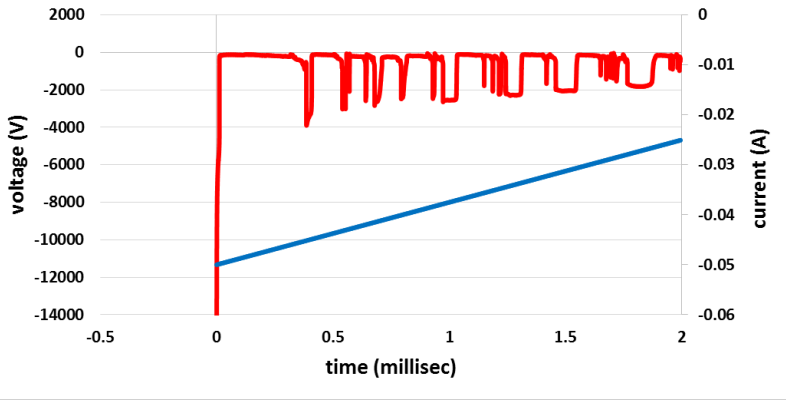

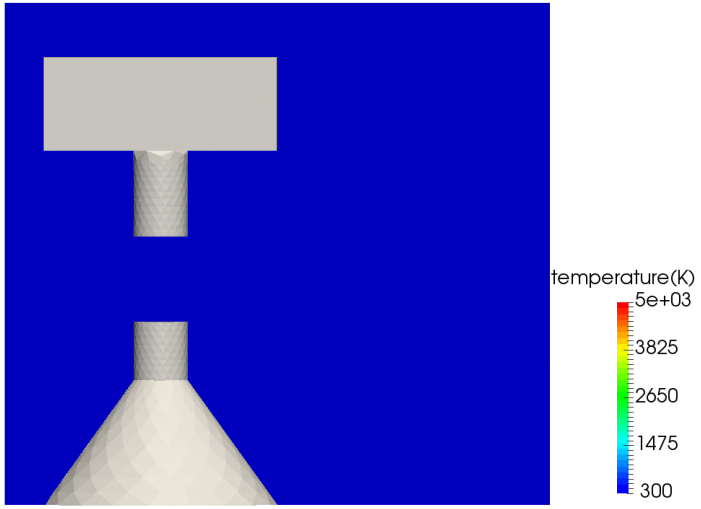

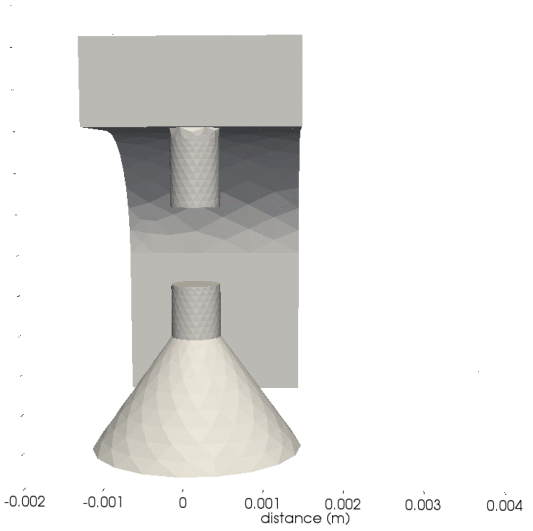

- Arc stretch increases with increasing cross flow velocity

Pressure = 500 kPa, Cross flow velocity = 8 m/s

- First re-strike event at 0.5 ms
- Re-strike voltage -4 kV

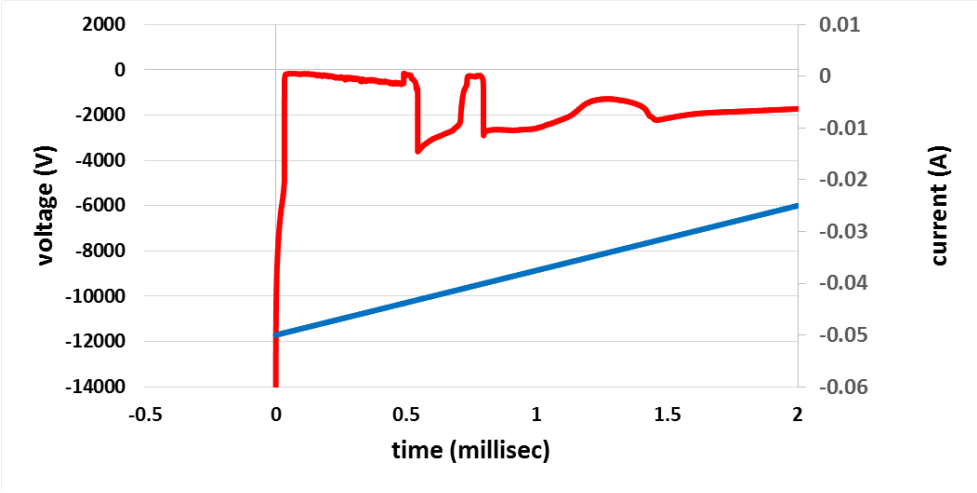

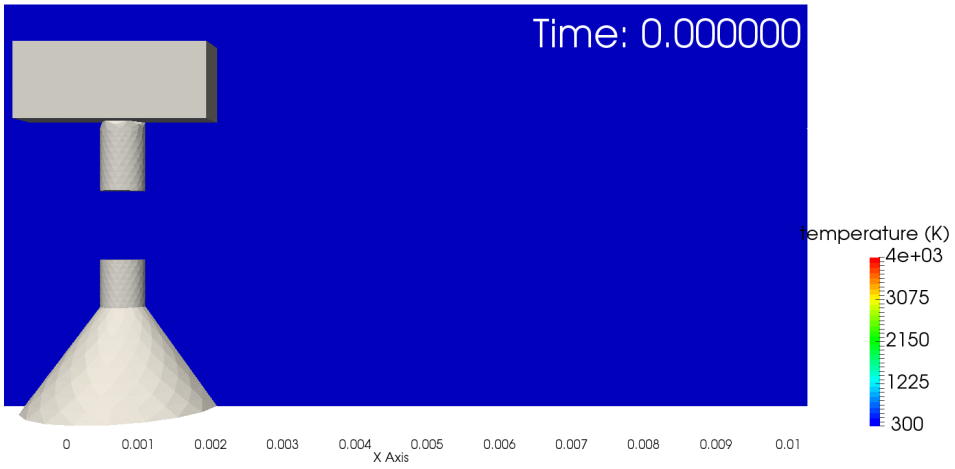

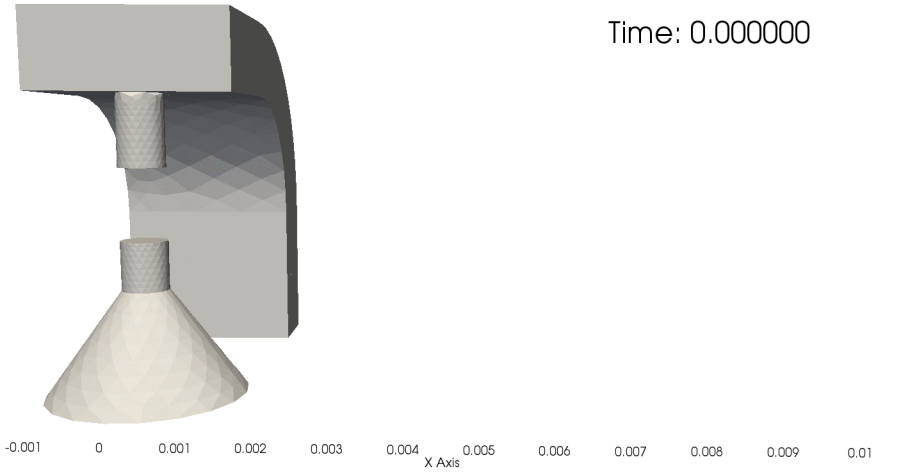

- Arc stretch increases significantly at higher pressures

Arc length before first restrike: Comparison with experiments

- Arc length before first restrike:
  - 100 kPa, 4 m/s
    Model result = ~ 3 mm
  - 100 kPa, 8 m/s
    Model result = ~ 5 mm
  - 500 kPa, 8 m/s
    Model result = ~ 9 mm

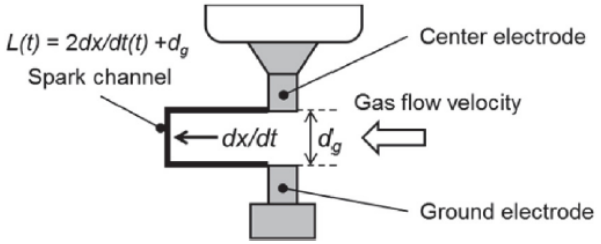

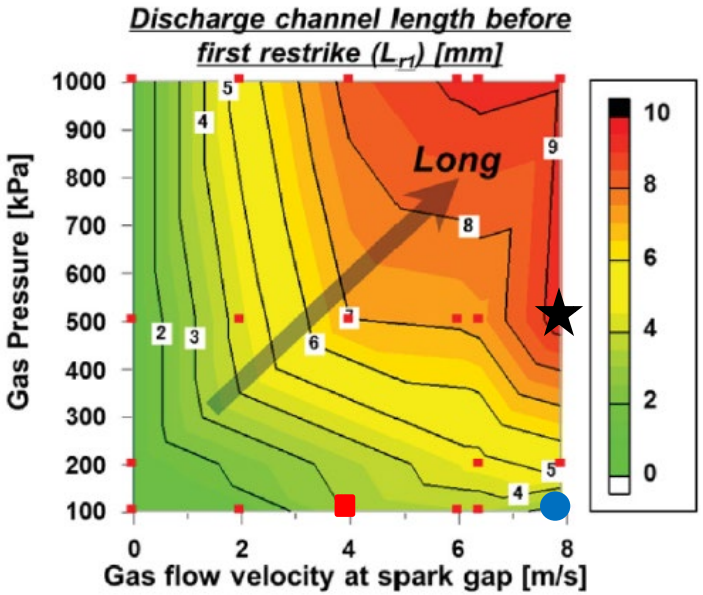

Image Credit: Shiraishi etal, SAE International 2015

- Good agreement between simulation and experiment predicted arc length

Example: SSPP based wide-area plasma ignitors

Kim, Pederson, Sharma, Subramaniam, and Raja, J. of Appl. Phys. 53, 265203 (2020).

SSPP based wide-area ignitors

- Plasma kernel size determines success of combustion ignition
- Spoof Surface Plasmon Polariton (SSPP) phenomena provides an approach for generation of non-equilibrium plasma over a wide surface area at high pressures

Surface Plasmon Polariton (SPP)

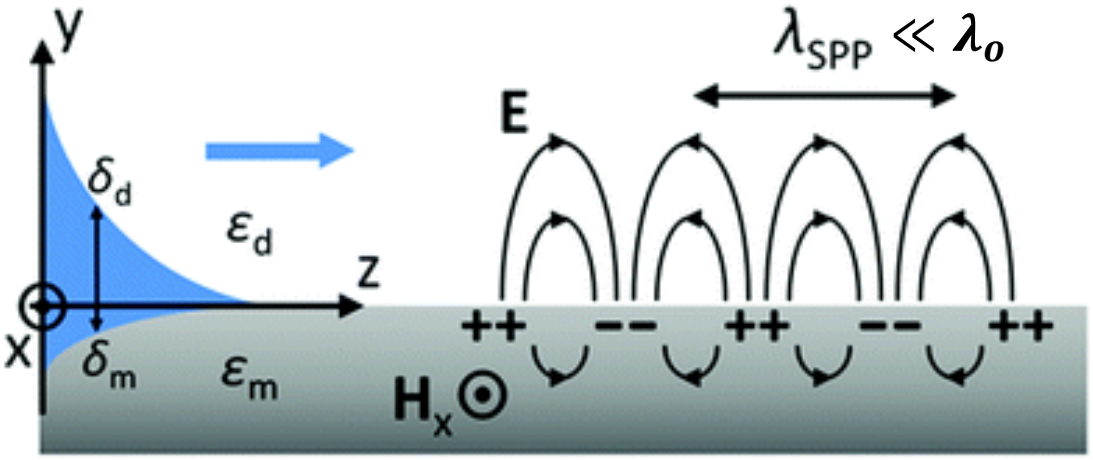

From: Smith., et al.

Drawbacks of classical SPP:

- Operating frequencies too high

High SSP limit frequencies are not practical

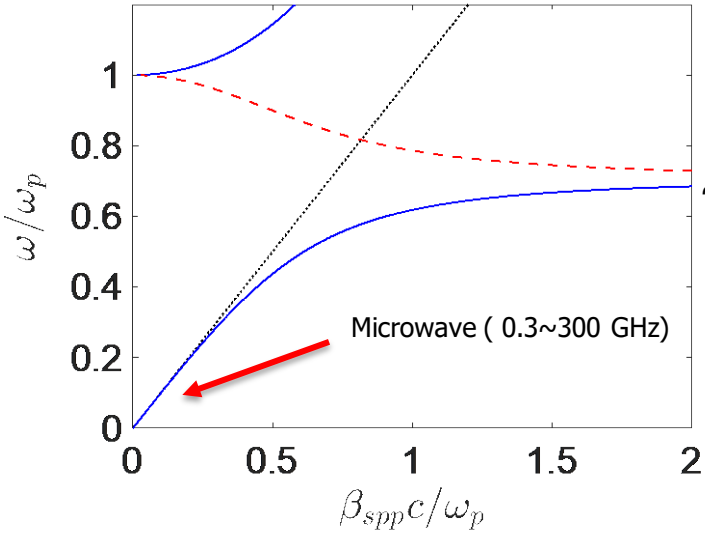

From: Maier

Spoof Surface Plasmon Polariton (SSPP)

- SSPP is an artificial excitation of surface wave mode that imitate SPP
- SSPP operates in microwave regimes, where SPP is inactive
- SSPP excitation: hybrid of cavity and surface wave modes

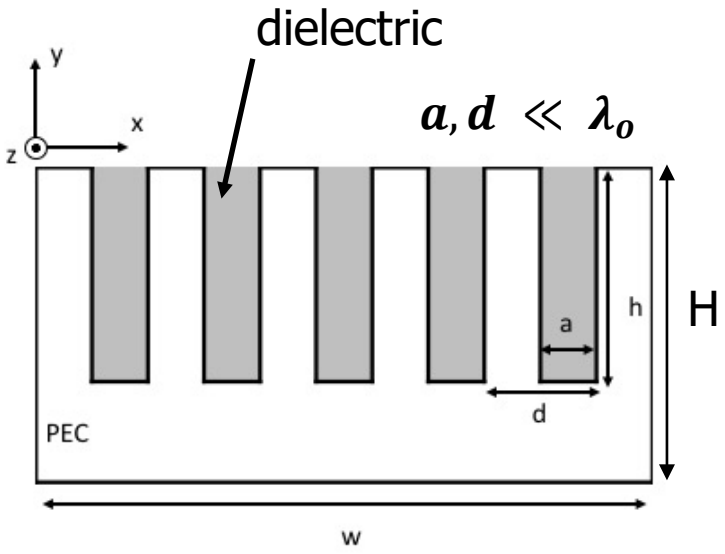

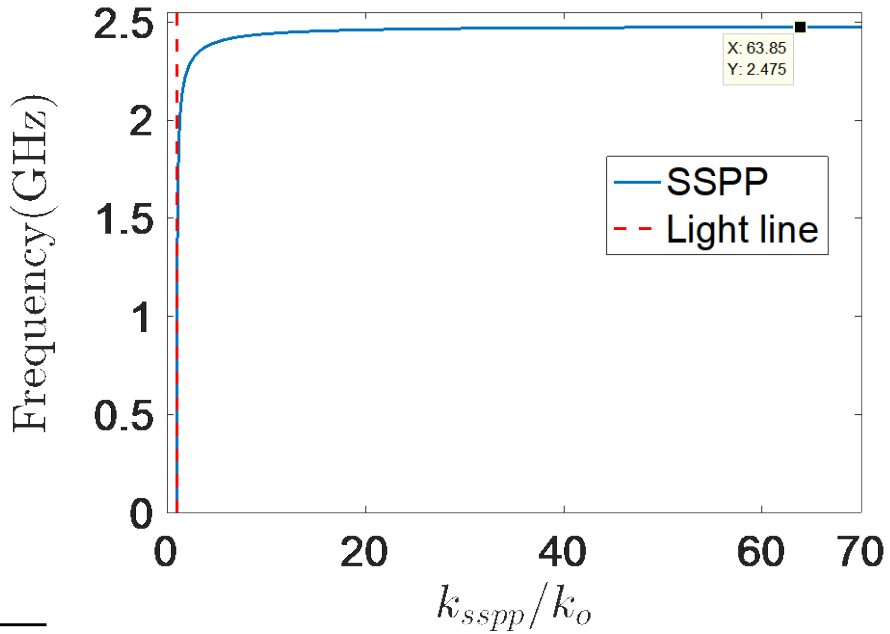

- Dispersion relation:

$$k_{sspp} = k_o \sqrt{1 + \left(\frac{a}{d}\right)^2 \frac{1}{\varepsilon_2} \tan^2(\sqrt{\varepsilon_2} k_o h)}$$

Computational Model

Maxwell's equations

- Helmholtz Decomposition
  - $\vec{E} = \vec{E}_m + \vec{E}_s$

- Electromagnetic field

$$\varepsilon \frac{\partial}{\partial t^2} \vec{E}_m + \frac{e^2 n_e}{m_e} \vec{E}_m + \frac{1}{\mu} \vec{\nabla} \times \vec{\nabla} \times \vec{E}_m = \bar{v} \vec{J}_e$$

$$H_0(curl; \Omega) := \{ \vec{u}: \vec{u} \in L^2(\Omega), \vec{\nabla} \times \vec{u} \in L^2\ (\Omega)\ \ , \vec{u} \times \hat{n} = 0\ on\ \ \partial\Omega \}$$

- Drude model for plasma:

$$\frac{\partial \vec{J}_e}{\partial t} = \frac{e^2 n_e}{m_e} \vec{E}_m - \bar{v} \vec{J}_e$$

$$\bar{v} = n_b \bar{g} \sigma, \qquad \bar{g} \propto \sqrt{T_e}$$

- Spatial discretization: FEM
- Temporal discretization: Newmark-β

49

Meta-surface configuration

- We introduce a dielectric layer over the meta-surface

I. Confine the local edge effects inside the dielectric.
II. More uniform EM energy distribution

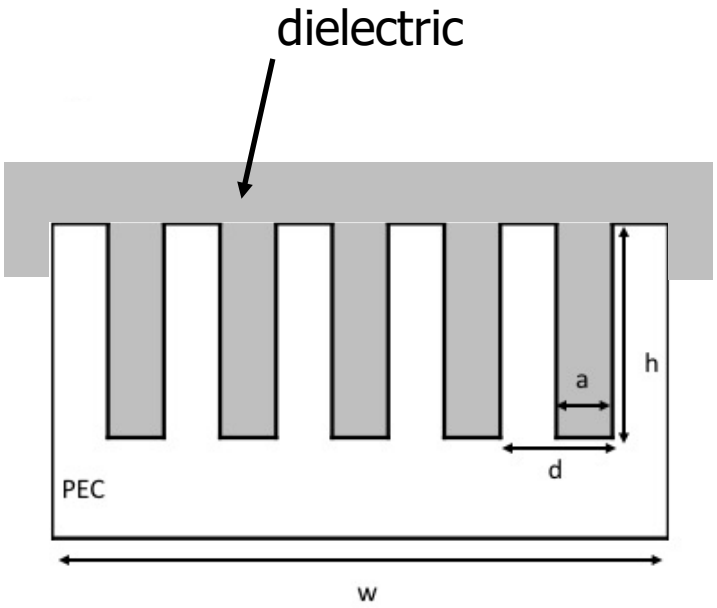

Dimensions
w = 0.95mm
a = 50μm
d = 100μm
h = 15.5mm

Resonance frequency determination : Broadband EMwave simulation

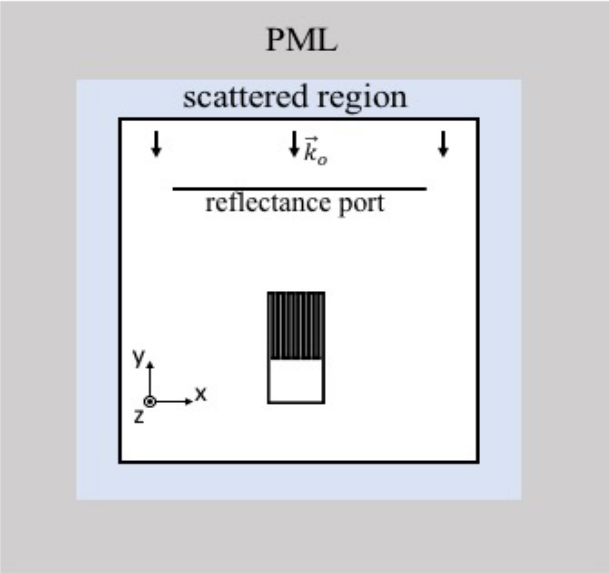

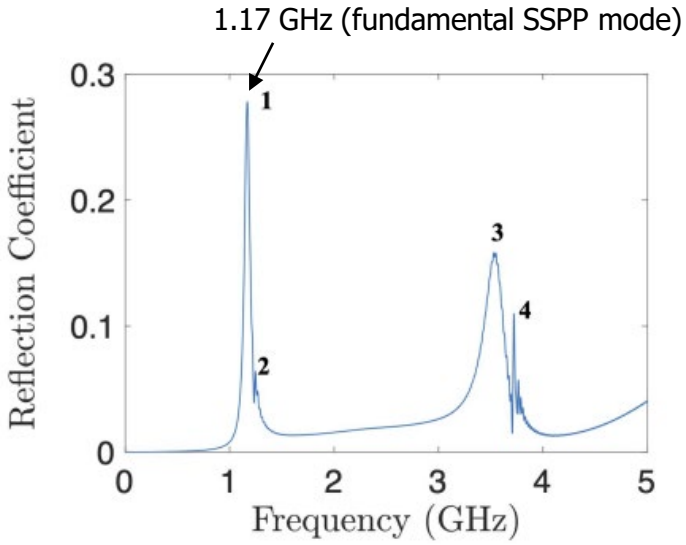

- Resonance frequency (Fabry-Perot like resonance) of the finite meta-surface.
- Fundamental mode
- Single node excitation

- EM wave pulse on for 19 ns

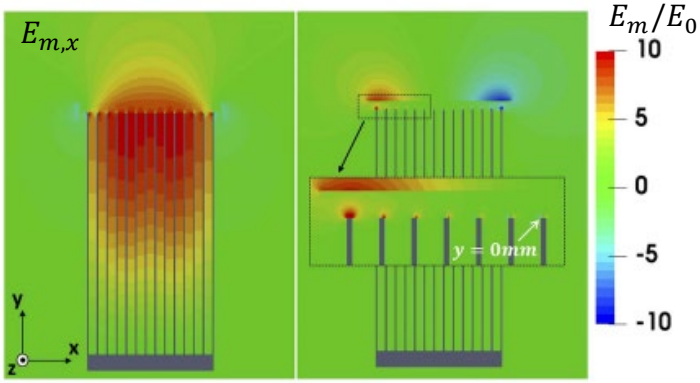

Discharge structure for 1.17 GHz excitation

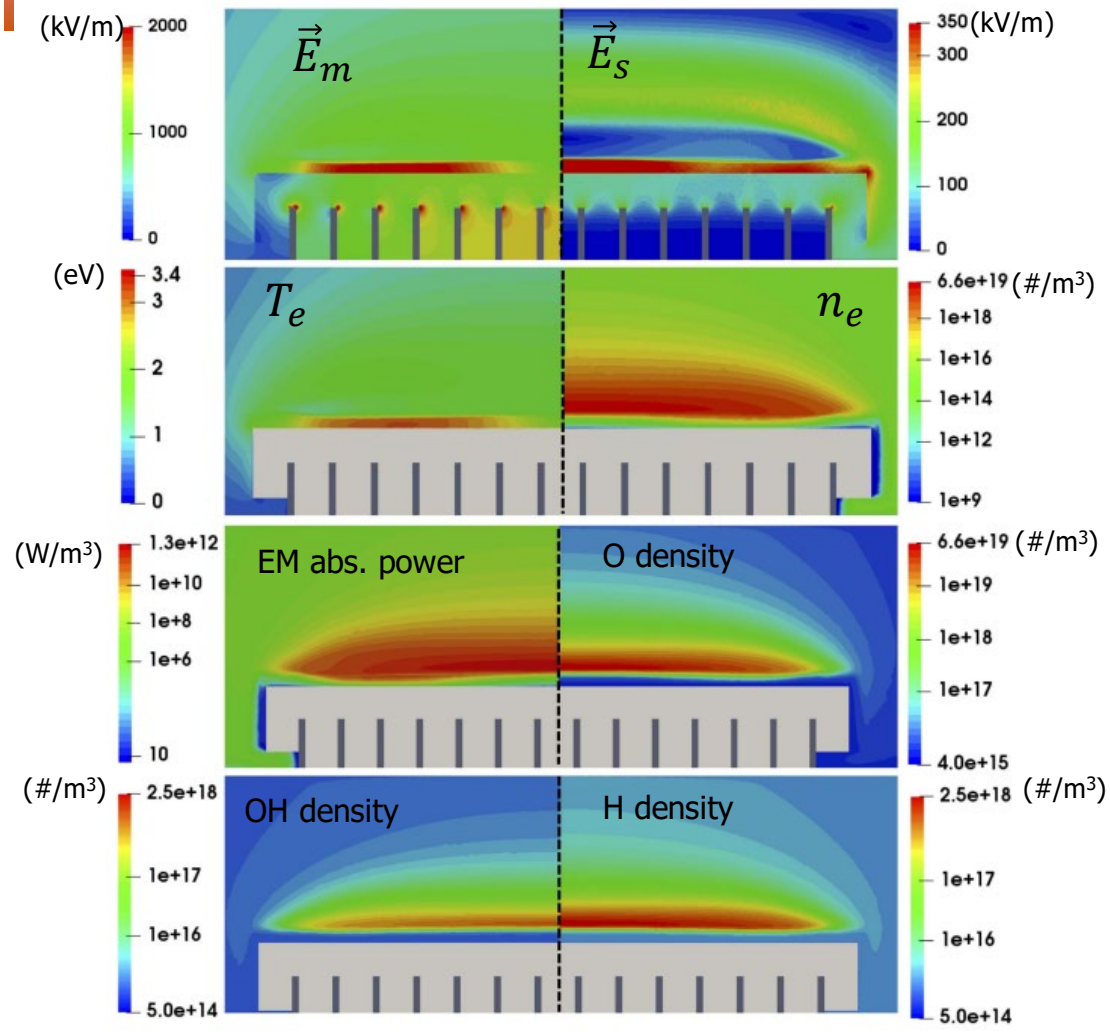

- Discharge at 8.8 ns after wave ON

Combustion ignition from SSPP

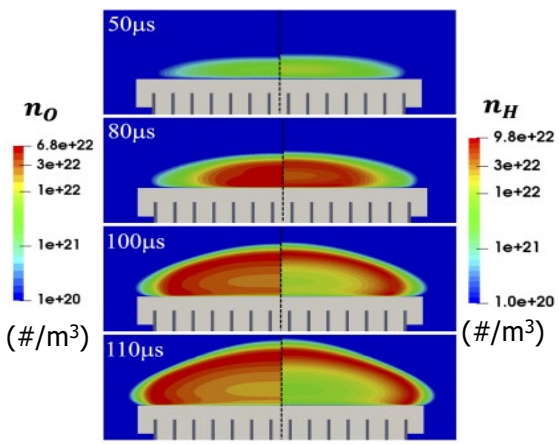

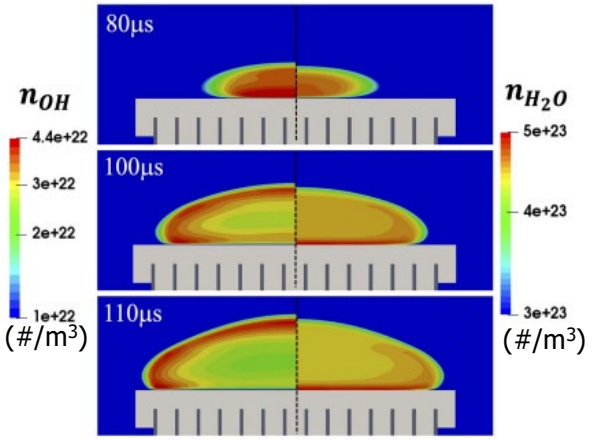

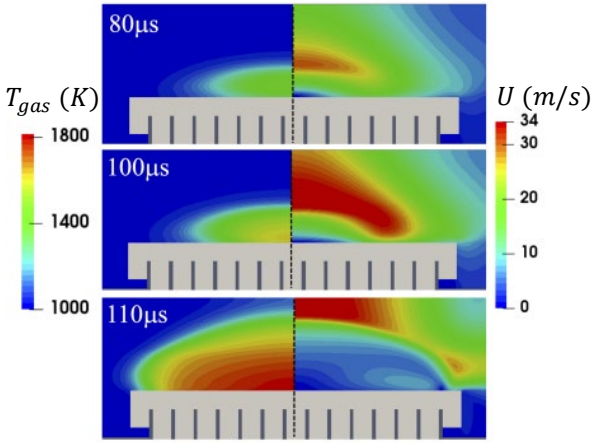

Gas properties at center above metasurface

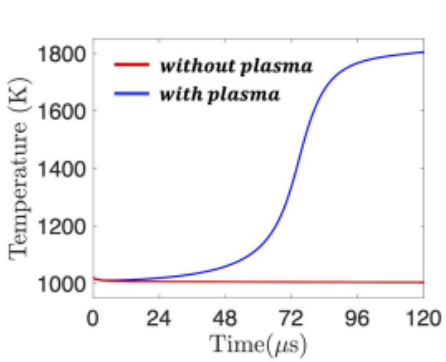

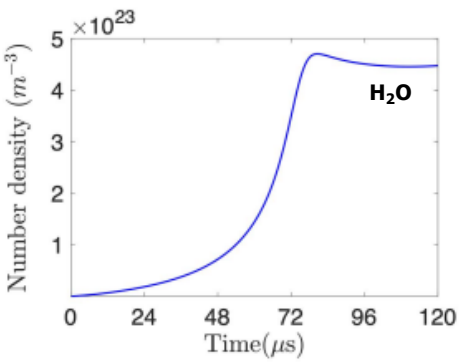

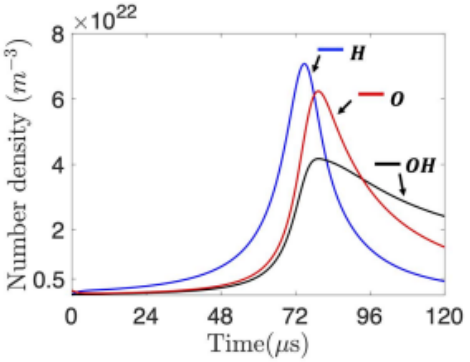

Summary

- Modeling and computational simulation of cold and thermal plasma discharges is now sufficiently mature that a variety of discharges can be simulated with reasonable accuracy with the same model

- Studied high pressure (atmospheric and higher) discharges in Single electrode corona, Coaxial electrode streamer, Pin-to-Pin streamer, and arc plasmas

- Developed and demonstrated concept for SSPP-based wide-area surface plasma ignitor

End of Presentation